# Detection of Tunnel Waves

**Funded by DARPA**

# Final Report

**April 30, 2010**

Technical Point of Contact: Valeri Korneev

Mailing Address: 90-1116, 1 Cyclotron Rd., Berkeley, CA 94720

Telephone: (510) 486-7214, Fax: (510) 486-5686,

Electronic mail: vakorneev@lbl.gov

Participants:

Lane Johnson

Thomas Daley

Seiji Nakagawa

All at Lawrence Berkeley National Laboratory

**Table of Contents**

## Summary

The results of modeling and field data analysis suggest that use of resonance seismic emission can solve the problem of tunnel detection and become an easy-to-use technology. Human activity in the tunnel can be detected as well. The necessary steps towards completion of such technology are suggested.

## Sites for the fieldwork

During the first phase of the project a search of potential targets for field data acquisition was performed. We considered the WWII military underground facilities in Marin Headlands, abandoned mines in Black Diamond Mines Regional Preserve, and a Bld46 adit (A46) located on LBNL's territory.

Marin Headlands tunnels and underground facilities (Figures 1-4) were not accepted as targets because of their large sizes (usually more than 4 meters in diameter), heavy and thick concrete armor (not typical for objects of interest) and a strong ambient noise coming from a nearby ocean coast line.

Black Diamond Mines present a significant interest for the project goals. While there is no mining activity there, they are still in good shape and accessible. This area is located 40 miles from the Lab and has many tunnels giving a variety of choices (Figures 5-6). Black Diamond Mines can be considered as a potential object for data collection for the next stage of the project.

LBNL and DARPA agreed that Bld46 adit (Figure 7) is the best choice to achieve the project's goals, where the main field work will be concentrated. A46 was originally built in nineteen forties in order to supply water for the city of Berkeley. The exact length of the adit is unknown because after 120' from the entrance the adit had collapsed. In the 60-s the original wood liner of the adit was enforced by steel frames and 10 cm thick shotcrete. Adit is horizontal and goes into a steep 35-25 degrees hill. The hill is mostly covered by soft soil with unknown thickness and has several bedrock outcrops composed of shales (Figure 8). A46 has a symmetrical trapezoidal shape having 4 ft at the base, 3 ft. at the top and 7 ft in height. More detailed history of A46 can be found in the Attachment 1.

## Numerical modeling

Computations were done using PC desktop computer with 2 Intel quad-core processors and 32 Gb memory size. This configuration allowed running 3D fully elastic finite-difference code for the models up to 800x800x800 grid size. Parallelization was implemented automatically through Intel Visual Fortran compiler.

The goal of the modeling was to provide some clues about resonance wave excitation in the void objects and explain the obtained field data. In the original publication (Korneev, 2009), the resonance emission was observed for a barrel filled with water and placed in a packed sand with both propagation velocities being smaller than P- velocity in the water. It is not clear yet, which waves generated resonances and whether or not similar resonances can be excited in the tunnels filled with air.

The model consisted of a homogeneous block 15m x 15m x 15m with a cylindrical pipe directed along x axis. The computations were done for four profiles with 70 data points each: A - going across the cylinder's center wall along y axis, B - at 6 m above the cylinder y axis and parallel to it, C - parallel to x axis right above the cylinder, and D - a circular profile of 5 m radius and co-centered with the cylinder (Figure 9). The parameters of the elastic embedding medium were Vp=500 m/s, Vs=250 m/s, density = 2 g/cm$^3$. The sound velocity in the air was 330 m/s. The density of the air was artificially high and equal 0.1 g/cm$^3$ because of the FD code stability issues.

During the numerical modeling we changed the cylinder radius, source type and position, cylinder inner filling, model size, and the source frequency content.

Figure 10 shows the trace at the source and its amplitude spectrum for a cylinder with 1 m radius filled with air, when a p- plane wave is generated at the source. Similarly to the barrel case, the source energy dominates in the record. The traces for all four profiles are shown on Figure 11 where long lasting resonance wave is visible. These waves become even more visible when the first strong arrivals are muted (gated) (Figure 12). Note the "hyperbolic" moveouts for the profile B.

Stacked autocorrelation spectra computed for gated traces of the profile B reveal a set of sharp resonancepeaks (Figure 13). Field snapshots of the late arrivals show surface waves propagating along the cylinder wall and circular waves (resonance emission) carrying energy away from the object (Figure 14), while in the y=const. section the waves propagate out without any significant changes in phases along x direction. How significant is the fluid (air) presence in the void? Figures 15-18 suggest that in absence of the fluid the resonance emission is still present in data, in this case attributing this phenomenon to the Rayleigh-type waves. Decrease of the cylinder radius predictably shifts the peaks positions to the higher frequencies (Figures 19-20). Use of a plane wave (Figure 21) reduces amount of excited peaks compare to a point source (Figure 17).

Increase of the void radius excites more low-frequency harmonics (Figure 22). To make sure that the observed peaks are not the results of some numerical artifacts the data for the voids were compared with the data for the purely homogeneous model in the late (after 0.2 s) arrivals (Figures 23-24). Also the grid size of the mesh was changed by the factor of two. The results of comparisons validated the used approach. Same models were used at a lower (seismic) frequency range (Figure 25). The results (figures 26-27) showed that the same (realistic) models for the tunnel can excite resonances at frequencies below 100 Hz.

## Fieldwork

The fieldwork in the adit was preceded by a series of safety testing and training. The adit has a history of a mercury spill and small intensity radioactive material placement. The test results for the chemical and radioactive contaminations were negative. The adit also was examined by structural engineers to ensure its safety as it was required by Lab's H&S officers. The LBNL' team had gotten the fall protection training because of the need to work on a steep slope. During the drilling of the adit's wall (for accelerators mounting) a special gear and mask was used by an operator to prevent a respiratory damage. The entire crew was supplied by two-way radios, boots, hardhats, and protective glasses.

There were three field surveys Adit1, Adit2 and Adit3, in which Geode (Geometrics Inc.) 24 channel recording stations were used. The first day (Friday) was used for setting and testing while the actual data acquisition was done on Saturday to minimize noise coming from traffic. We recorded seismic waves on a surface by 24 channel lines with GC20DM OYO geophones. Inside the adit the recording was done using accelerometers (797L, Wilcoxon Research Inc.).

Water was applied to the soil in the vicinity of surface sources and receivers to improve coupling.

Adit1 (took place on 05/21/2009-05/21/2009) was a pilot survey aimed to measure the spectral content of the recordings and the noise level, when one geophone line with 5 ft spacing and ten accelerometers in the adit with 12 ft spacing were used (Figure 28). The geophone line was oriented orthogonally to the adit's central axis on approximately same elevation crossing the projection of the adit's axis at 90 degrees in the middle of the line. It was intersecting the tunnel axis at the far end of the supported part of the adit, which was along a paved path going across the slope. In that survey the noise content and the range of excited frequencies were evaluated. Two Geode stations were used for recording.

Adit2 survey (08/21/2009-08/21/2009) took an advantage of scheduled maintenance (shutdown) of the electrical power system in several buildings closest to the adit in order to provide minimum electrical and acoustical noises coming from nearby. This time one geophone line S1 was oriented uphill starting from the adit's entrance with 5 ft spacing. The other line S2 had the same position as in Adit1. Twenty accelerometers were used in the adit with 4 ft spacing (Figure 29). Three Geode stations were used for recording.

In Adit3 experiment (11/21/2009-11/21/2009) the S2 line was moved to the steep slope part intersecting the adit's central axis above the middle of the adit (60' from the entrance). Ten more accelerometers were added, so the adit was covered with 25 recording points along the wall with 4 ft spacing, and 5 extra accelerometers were used in addition to the existing from the linear profile to cover the perimeter of the vertical cross section at i9 position (Figure 30). Four Geode stations were used for recording. At the second half of the Adit3 all accelerometers were simultaneously recording 3C motion of ten points of the vertical cross-section at i9 position to record polarization of the waves inside of the adit. Multiple source excitation (16-20 times) was used for suppressing noise by stacking. At the surface three source points P1, P2, and P3 were located along the S2 profile next to receivers #5, #13 and #18. Excitation was done in West-East direction (parallel to the S2 profile), in North-South direction (parallel to the adit's axis, and vertically.

A sledge-hammer was used as an outside source hitting a wooden block normally and tangentially to the ground. The sledge-hammer and a hammer were used as sources inside of the adit hitting the adit's walls and the floor. In Adit3 survey a walking person was also used as a source, aiming to provide some clues for tunnel activity detection. Photos from Figures 31-33 provide an additional information about the field work setting.

## Field data

Recorded seismograms look quite repeatable (Figure 34), revealing direct P- and S- waves in both surface and adit receiver lines. Velocities of these waves were estimated as Vp=603 m/s, Vs=302 m/s from the geophone line and as Vp=720 m/s, Vs=410 m/s from the accelerometer line. Higher velocities in the adit

are likely the result of wave propagation in rock, whereas for the surface line wave propagation is affected by soft soil with variable and unknown thickness. Analysis of spectrograms (Figure 35) for shots in the adit reveal presence of frequency peaks at 86 Hz, 175 Hz, 235 Hz, and 275 Hz, which are distinct for adit line and can be also traced on the surface line. The interesting feature of the 86 Hz peak, is that in fact its value is changing depending on an accelerometer position. For source i21 (lower panel on Figure 36) the resonance happens at 90Hz at the adit entrance gradually decreasing to 86 Hz farther inside. If the source position moves away from the adit entrance (Figure 36) this effect vanishes. This resonance is of our primary interest because this is the lowest frequency which gives hyperbolic moveout (Figure 37), and therefore is likely connected with the adit. The causes of the frequency dependence on the distance along the adit will be discussed later. The value (86 Hz ) of this resonance changed to 89 Hz for the surveys Adit2 and Adit3. This temporal change can possibly be explained by variations in rock/soil water saturation. In the following we will call this resonancefrequency *A frequency* (AF) to avoid a confusion due to its variability. While during Adit2 the soil was dry, the othe two surveys took place after heavy rains. Local shales are very fractured and known for their high water storage capacity. The records also show other spectral peaks at lower frequencies, which however did not show obvious hyperbolic shape with one exception of human walk case, that will be discussed at the end of this report.

Ambient noise spectra for geophones (Figure 40) and accelerometers (Figure 41) show presence of many spectral peaks. However, there are no peaks in the range of 80-100Hz, which indicated that the AF is generated by the adit. AF clearly appears in data if a concrete base on the top of the hill (see Figure 30) is hit by a sledge hammer. However, in this case it is not clear if the source can be regarded as a surface source, because the base is connected with the adit via steel pipe.

Ambient noise (Figure 43) during Adit3 survey was very different than in the previous survey. It was much more intensive and had a different spectral content (Figures 44-45). AF was not visibly present in the noise. In the adit the excitation was done from the points i1, i9, and i17 (see Figure 30) where i9 projection on the surface was close to intersection of profiles S1 and S2. Example of geophone record from i9 location is shown on Figure 46. Early arrivals at the end of S1 are likely caused by fast waves propagating in the shotcrete casing of the adit. Example of accelerometer record from i9 location is shown on Figure 47. First body waves arrivals are dominant similarly to the case of barrel and to the results of numerical modeling. Figure 48 shows a trace recorded close to the intersection of tprofiles S1 and S2 from the source point i9. The resonanceemissions were searched in the gated traces (Figure 49, upper panel) where only late arrivals in 0.2 - 0.45 interval were left. Amplitude spectrum of bandpass (70 - 400 Hz) filtered traces reveal distinctive peak at AM (Figure 49, lower panel). Figure 50 shows the same trace without bandpassing. It has two more resonancepeaks at 10 Hz and 21 Hz. On a stacked spectrum (Figure 51) just 21 Hz peak survives. Acceleration data in Adit3 survey is rather noisy. Figure 52 (upper panel) shows an example of a trace recorded in the adit. After 0.04 s the signal becomes lower than the noise level. Gated late phases have many peaks including AF. Some traces which were within 10 ft from the source were clipping the signal (example is on Figure 53). Such things were not happening in Adit1 and Adit2 surveys. High noise level and higher recording gain could be a reason for this. Stacked accelerometer spectrum is shown on Figure 54. This spectrum contains AF peak, however it does not have the highest value. Spectrogram for the adit shot i9 (Figure 55) shows consistent presence of AF in geophones.

Unless specified separately, data shown in the next figures were pre-processed using the following procedures: raw traces were gated leaving just late arrivals after 0.2 s, then they were bandpass filtered above 60 Hz, and then traces were separately normalized to remove the effects of geometrical spreading and attenuation.

Spectral signatures of late arrivals show stability after comparing three sets of geophone data obtained from the same shot point after an hour of time difference (Figure 56). Values for resonancefrequencies obtained from different shot points stay the same, but relative peak values vary (Figures 57-58). Most effectively AF is excited from the middle point in the tunnel. Most effectively the resonancefrequencies were excited in the adit by applying the vertical hits, showing the same resonance frequencies from different source positions (P1, P2 and P3). Note that appearance of AF in the adit from surface shots reveals stability of resonancefrequency independently from the source frequency content. Similar behaviour was observed for other combinations of data: geophone data excited from three different positions (Figure 60), using three different source orientations (Figure 61), accelerometer data excited from the surface in horizontal direction.

Narrow band-pass filtering around AF for the shot i9 gave hyperbolic shape for the data on profile S2 (Figure 63) similarly as it was shown in the Adit1 survey (Figures 37-38). The same effect gives filtering around 21 Hz resonance frequency for shot i9 in the adit (Figure 64), and for vertical shot in P3 on the surface (Figure 65).

Numerical modeling of the adit with background velocities Vp=720 m/s, Vs=410 m/s, and density 2 g/cm3 was done for a point source placed in the point (7.5, 11.0,11.0) to avoid pure symmetry in order to excite more possible harmonics. The x=7.5 m snapshot at 0.2 s (Figure 66) shows propagation of Quasi-cylindrical waves coming from the adit. Figure 67 shows the same wave field in y=7.5 m section. Similarly to the field data scheme the recording profiles S1 and S2 were forming a cross with S1 profile oriented parallel to the adit's center axis and profile S2 oriented perpendicular to this axis. Raw modeling data are shown on Figure 68 (note a green lighted trace on S2 profile showing a big difference in amplitudes for the first and late arrivals).

Figure 69 shows just late arrivals after muting traces before 0.15 s. Figure 70 shows amplitude spectra of traces from Figure 69. An important feature of these computed spectrograms is constant values of frequency peaks positions. Another (surprising) feature is a strong variation of amplitudes for each peak with receiver position.

Comparison of the field and modeled data is shown on Figure 71, where stacked amplitude spectra of FD modeling are plotted on top of the data recorded in the adit and by geophones.

The highest peak on modeled data occurs at 88 Hz frequency, which corresponds to AF peak and present practically on all field data. Small peak at 22 Hz (Figure 72) might be related to the observed peak at 21 Hz (Figure 51). Figures 73-76 show narrow band-pass filtered traces with correspondingly 53 Hz, 88 Hz, 118 Hz, and 154 Hz resonance frequencies selected from modeled results for profile S2. All of the phase changes exhibit hyperbolic moveouts, indicating a presence of a localized contrast object. Introduction of a slope in the model (Figures 77-78) brought some changes in the correspondent spectrograms. Resonance peaks showed some variation in frequencies as a function of their position in the profile (Figures 79-80). For example, a 27 Hz peak on a first trace of profile S1 end up at 29 Hz value in the last

receiver, which is closest to adit's "entrance" (Figure 80). This is consistent with similar behavior of the AF peak observed in Adit1 survey (see Figure 36).

Finally, the human activity in the adit was recorded in the field experiment. A person was walking while recording for 12 seconds long. Figure 81 shows comparison of noise and "while walking" records bringing a definite conclusion that walking in the adit can be detected. Narrow band-pass filtering of these records around 13 Hz frequency gave a clear hyperbolic signature (Figure 82).

## Discussion

Modeling results suggest that resonance waves can exist in tunnels, and that these waves can be excited and recorded remotely due to seismic resonance emission. In absence of very complex surface topography the resonance frequencies stay constant in their values, which brings a possibility of using pattern recognition techniques for tunnel parameter evaluations.

Field work environment used in the project had been rather complex which involved several factors, such as:

1. Complex geology (see map from Figure 8) where two different types of rocks co-exist in nearby vicinity and most likely generate extra unwanted reflections. Contact between soft soil and bedrock is a complex and generally unknown. Some sensors were planted in outcrops.

2. Complex topography, that likely generated extra reflections and affected effective rock parameters surrounding the adit.

3. Uncertain quality of contact between shotcrete and rock could affect the data.

4. Nearby buildings were likely extra reflectors for the recorded waves superimposing the waves coming directly from the adit.

5. Working fans, electrical motors and machinery in nearby buildings.

6. Closeness of multiple electrical power lines.

7. Close open entrance of the adit and the vertical steel pipe served as traps and conductors for various acoustical noises.

8. Noise coming from the water flowing in a drainage channel under the adit's floor.

Despite of these conditions AF peak is present in practically all data and for some shots a correspondent hyperbolic moveout was observed. Similar moveout was also observed for 21 Hz frequency using sources both in the adit and on the ground. Unlike the barrel case the observed hyperbolas are not ideal and have some phase shifts along the profile. This observation has several likely explanations. First, the discontinuous moveout can be always observed only for the fundamental mode when the object radiates isotropically in all directions. All other modes cannot radiate purely circular waves with a constant phase. Modeling data confirms this statement. Second, in a complex environment we simultaneously record interference between waves coming from the target object and waves reflected from other heterogeneities. Surface data recorded in 2D should allow separating those waves during 3D imaging. Third, traveltimes

(phase patterns) can be affected by variable velocity. Therefore, the obtained "hyperbolic" patterns look realistic and should not be a burden for imaging. Finding of hyperbolic signatures in data is not a required step for imaging, but rather serves as an indicator that such imaging will be successful.

Modeling showed a small peak at 22 Hz which might be related to the observed peak at 21 Hz. The difference in their amplitude can be explained by higher attenuation of high frequencies in rocks. Numerical modeling did not use any attenuation mechanism. Also, this peak had highest amplitude when the source was applied to the adit's floor. In the modeling we had used an external source simulating excitation of resonances from the surface.

High noise level did not allow studying polarization of tunnel wall motion.

Modeled data for the adit model gave a good fit to the observed frequency peaks above 50 Hz. AF peak is the most prominent feature of the modeled spectra. This suggests feasibility of modeling approach in developing of tunnel detection methods.

Tunnel activity (walking inside of the tunnel) data showed striking difference compare to just the ambient noise pattern. The records indicate that besides a detection of such activity it is possible to determine a location of the tunnel.

## Conclusions

Observed and modeled data are consistent and indicate the possibility of tunnel detection using seismic resonant emission.

Specially developed software would allow a real-time tunnel detection and location.

Human activity in a tunnel is detectable using seismic waves.

## What is next

Before the tunnel detection can become an easy-to-use technology, several problems need to be solved.

1. Imaging of the tunnel in 3D. So far, in all applications (the barrel and the adit) the main seismic line was oriented across the object's central axis, making detection especially easy, because it can be done in 2D. In practice we would not know the tunnel orientation, which should be determined in the process of imaging.

2. Optimal source and sensor array requirements need to be formulated depending on the expected tunnel parameters.

3. Use of ambient noise for tunnel detection needs to be studied.

4. Simple and automated background velocity evaluation needs to be developed and tested, so in practice that can be done by an operator without special knowledge about seismic wave propagation.

5. Use of wireless sensors (of a base of MEMs) would simplify the practical applications.

To solve these problems, several (at least two, in different geological environments) more 2D data sets need to be collected for known existing tunnels, and using both active sources and ambient noise. Black Diamond Mines seem like an ideal site for the next fieldwork, because it provides an access to a variety of tunnels with different depths, diameters and equipment. The collected data, complemented by the results of numerical modeling will serve as a benchmark for the tunnel technology development, which will lead to development of a easy-to-use software allowing real-time robust tunnel detection.

## Figures

**Figure 1.** Marin Headlands drainage tunnel.

**Figure 2.** Marin Headlands. Tunnel under 101 freeway.

**Figure 3.** Marin Headlands. Battery Townsley tunnel.

**Figure 4.** Marin Headlands. Fort Barry tunnel.

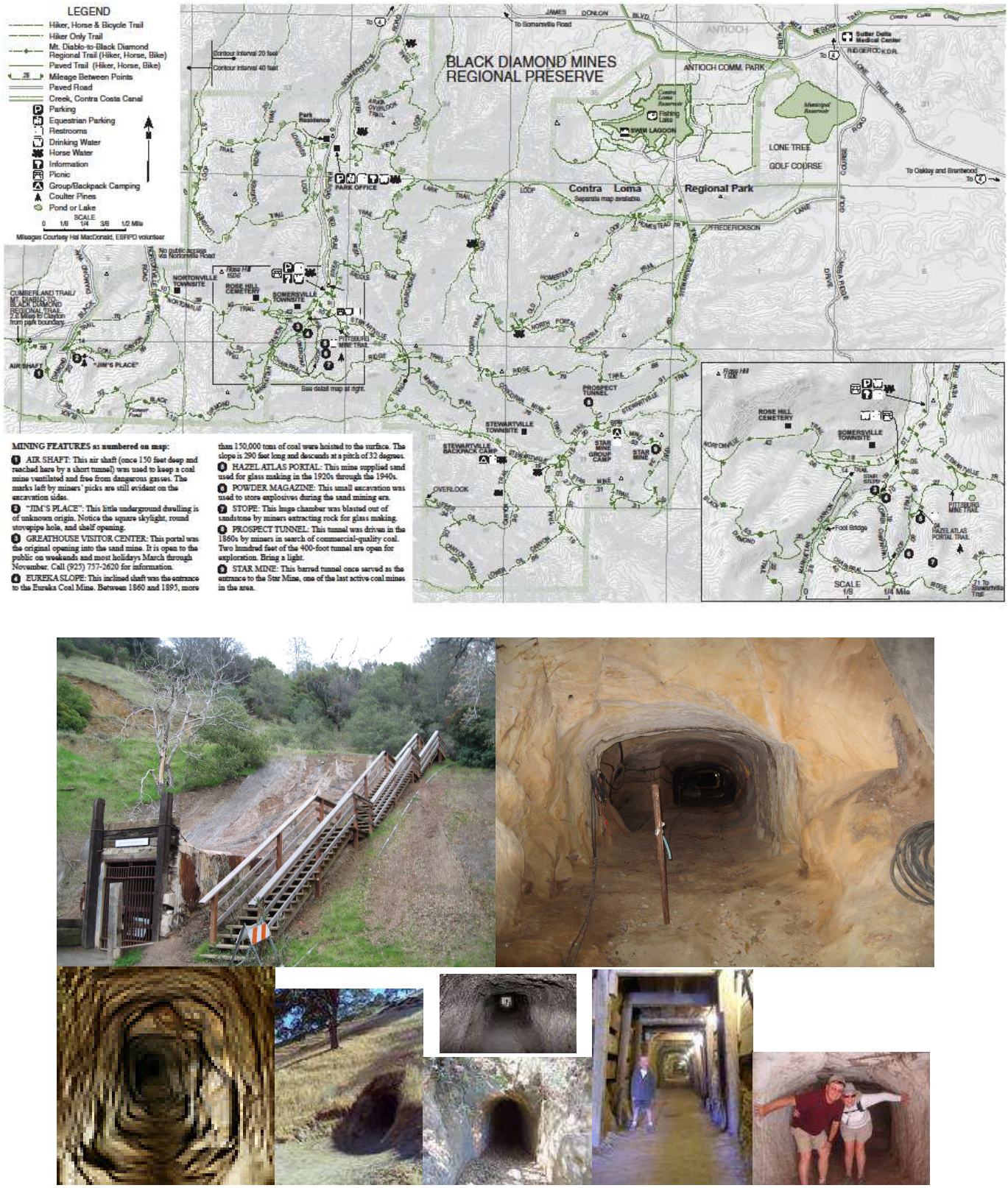


**Figure 6.** Examples of different tunnels at Black Diamond Mines Regional Preserve.

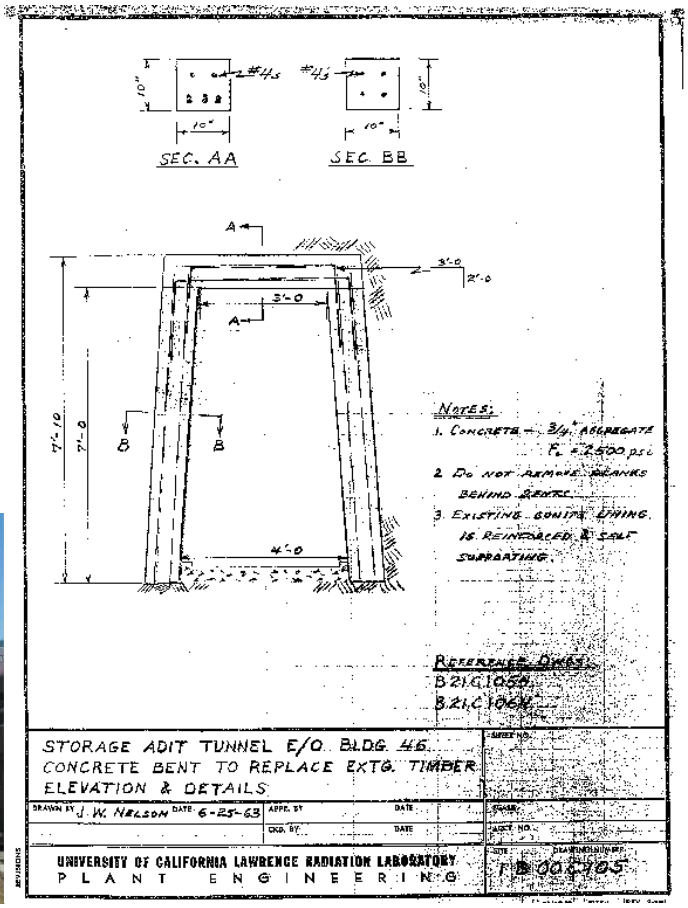


**Figure 7.** LBNL Bld.46 adit. Inside view (upper left panel), outside view (bottom left panel). The adit's entrance is in the low right corner. The right panel shows drawing of adit in 1963 when it was reinforced.

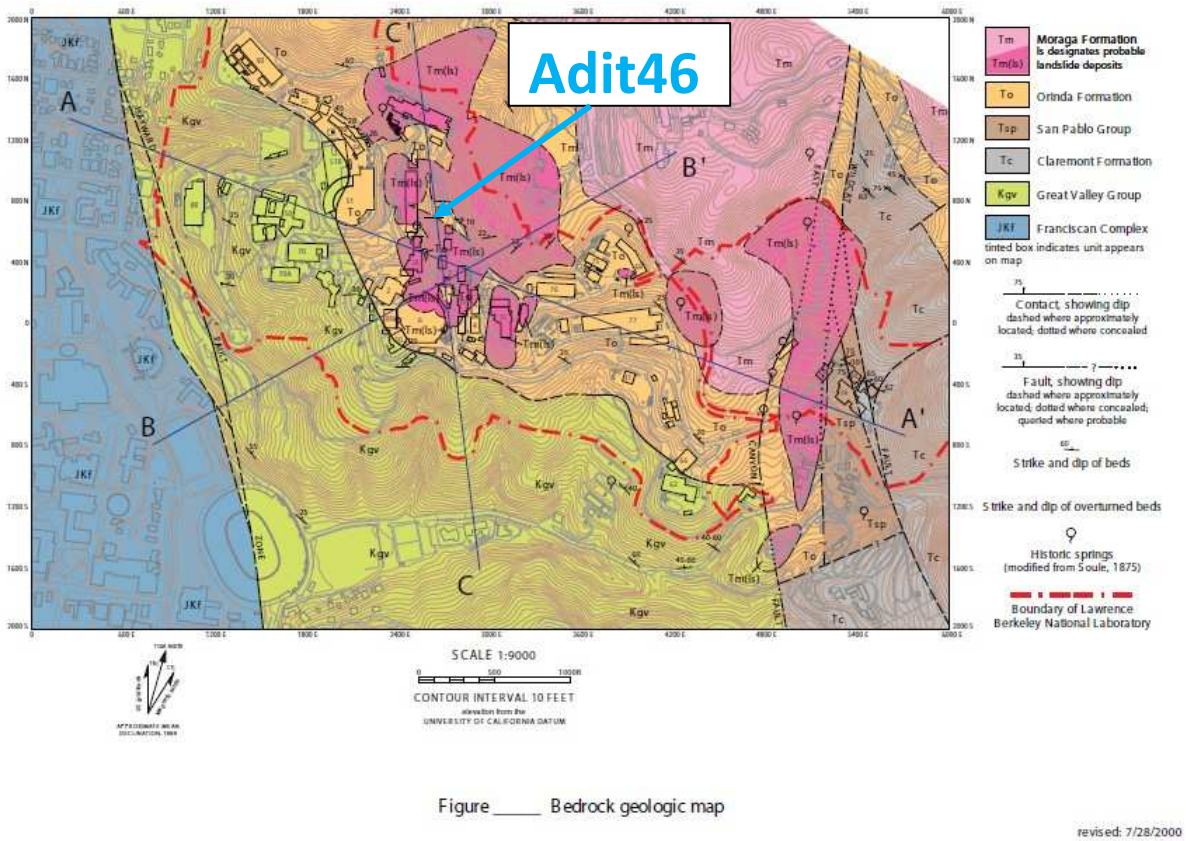


**Figure 8.** LBNL's site geological map with Bld46 adit location.

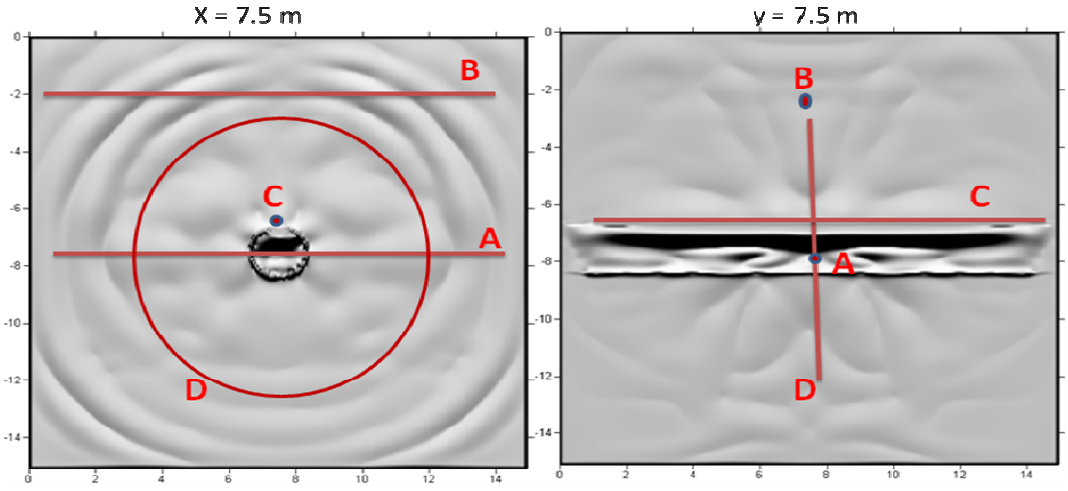


**Figure 9.** Frames and profiles for 3D FD modeling of tunnel waves.


**Figure 10.** Trace record at the point source (upper panel), and its amplitude spectrum (lower panel).

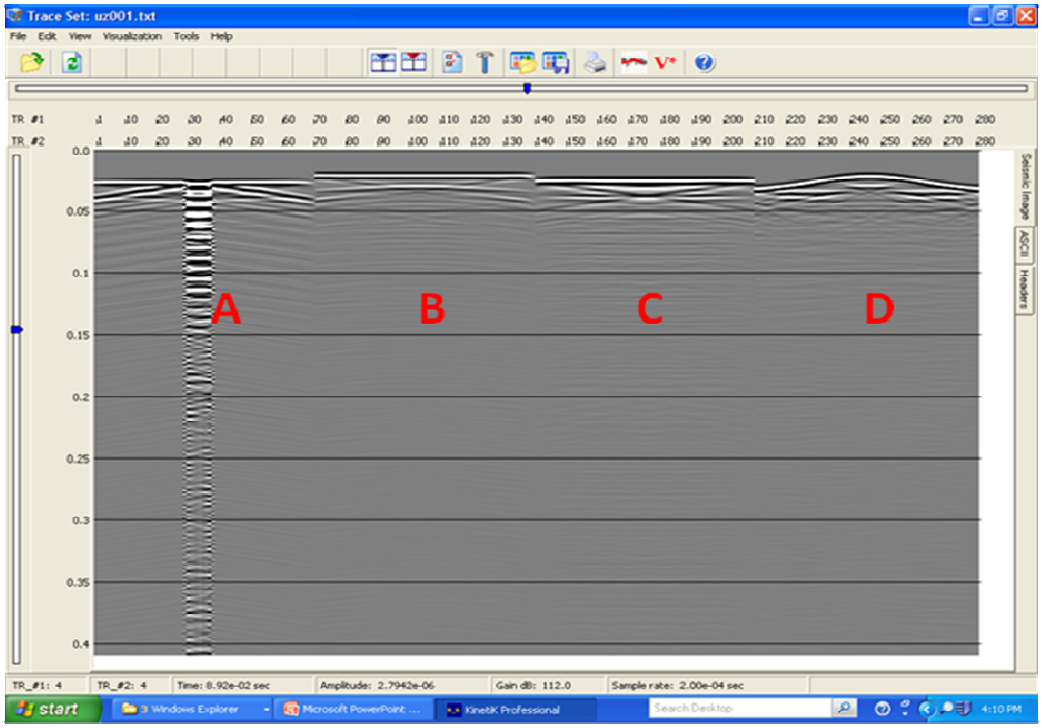


**Figure 11.** Traces recorded for a cylinder with 1 m radius filled with for a plane wave source.

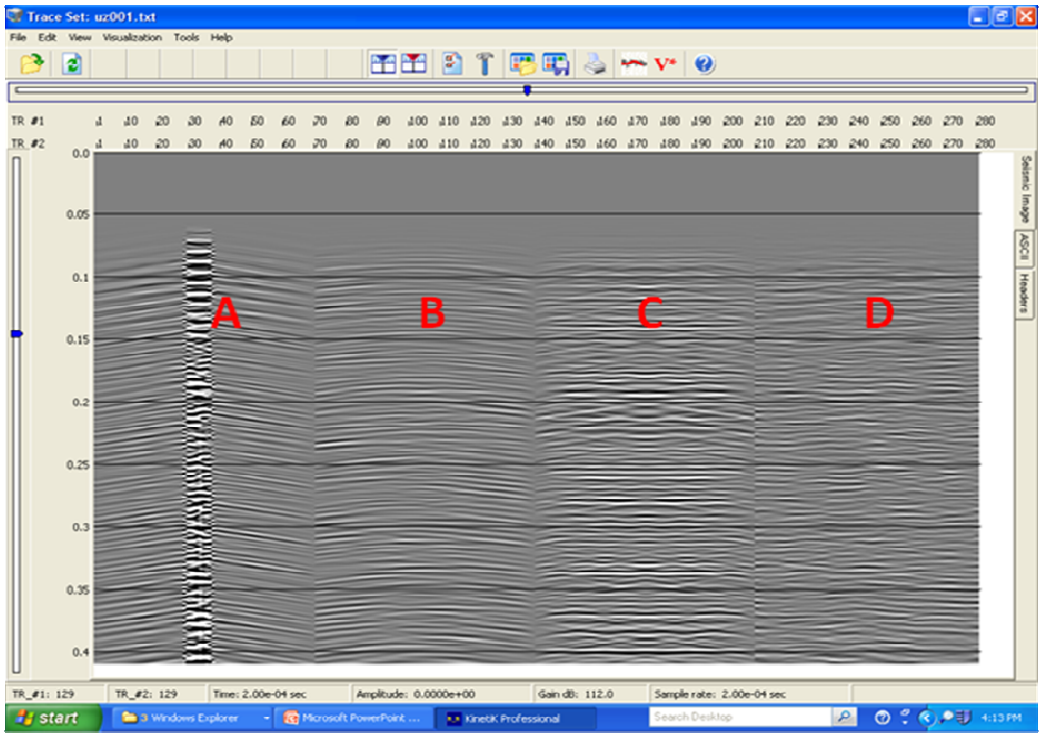


**Figure 12.** Same as on Figure 11 with first arrivals muted. Visible are durable oscillations of the resonant emission.

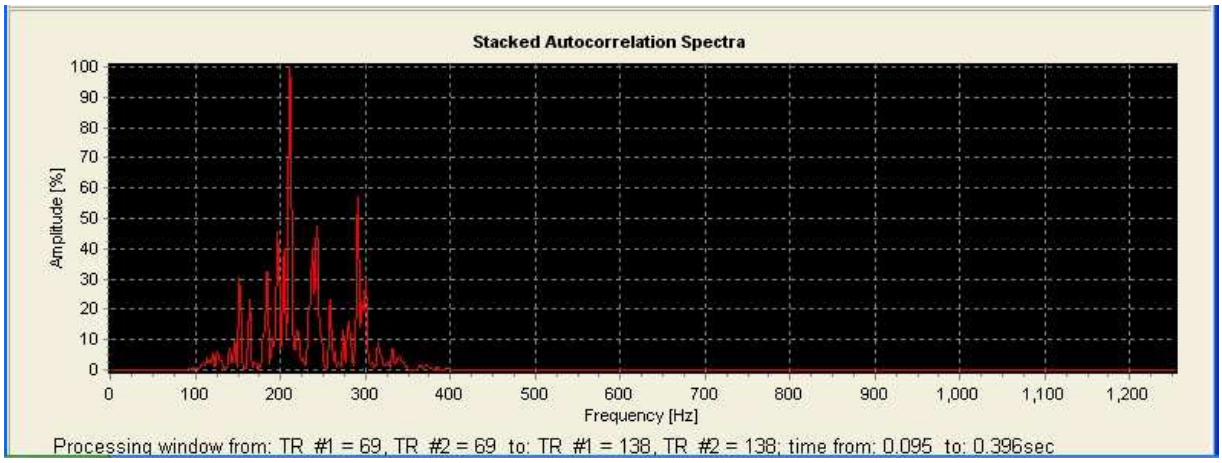


**Figure 13.** Stacked autocorrelation spectrum of the traces (B) from Figure 12.

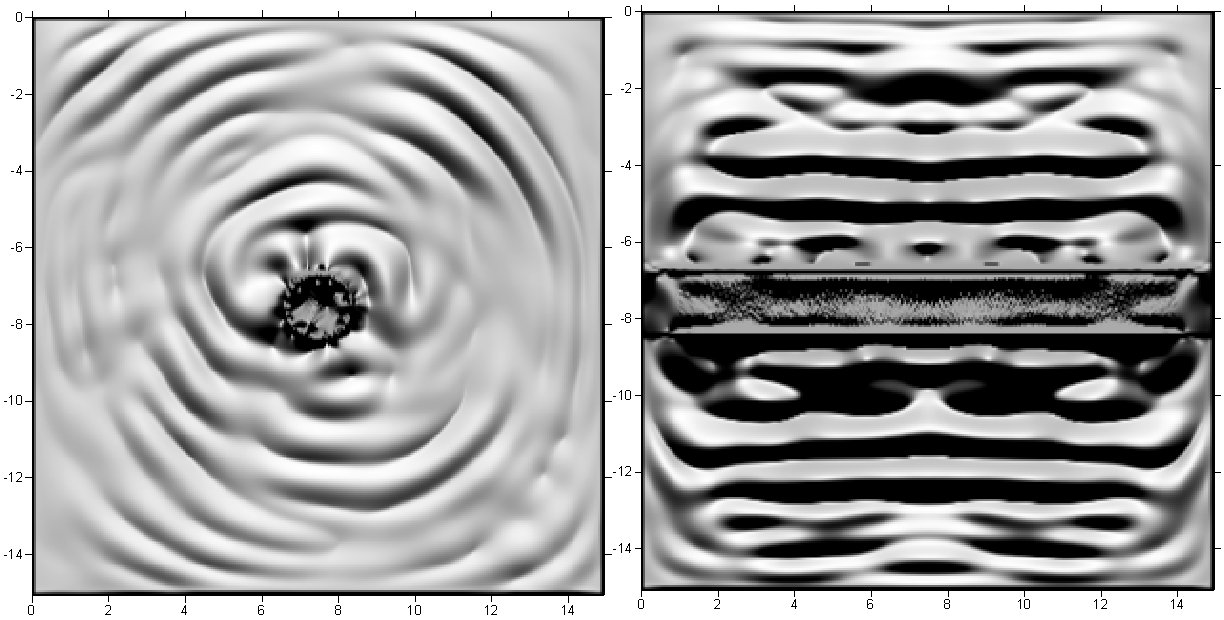

**Figure 14.** Sesmic field snapshots for the case of Figure 11 at 0.2 s. Resonance emission waves propagate as quasi-spherical waves away from the cylinder (left panel) while for y=const. the waves phases are almost constant along the x axis (right panel).

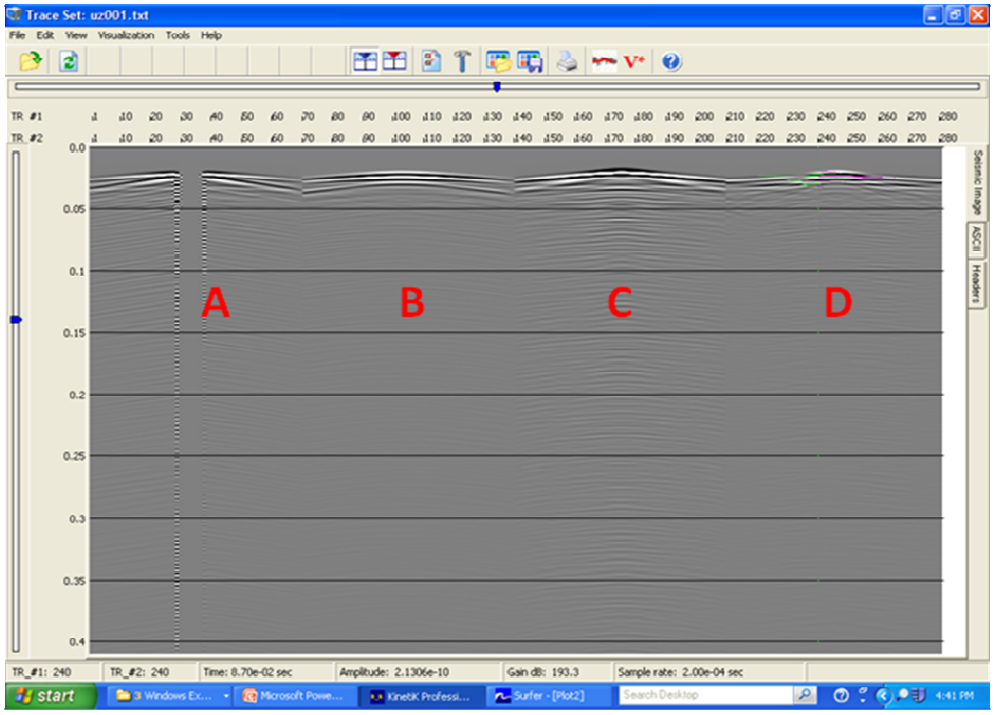


**Figure 15.** Traces recorded for a void cylinder with 1 m radius for a point-pressure source. Despite the absence of material inside of the object, the resonance waves dominate the late arrivals.

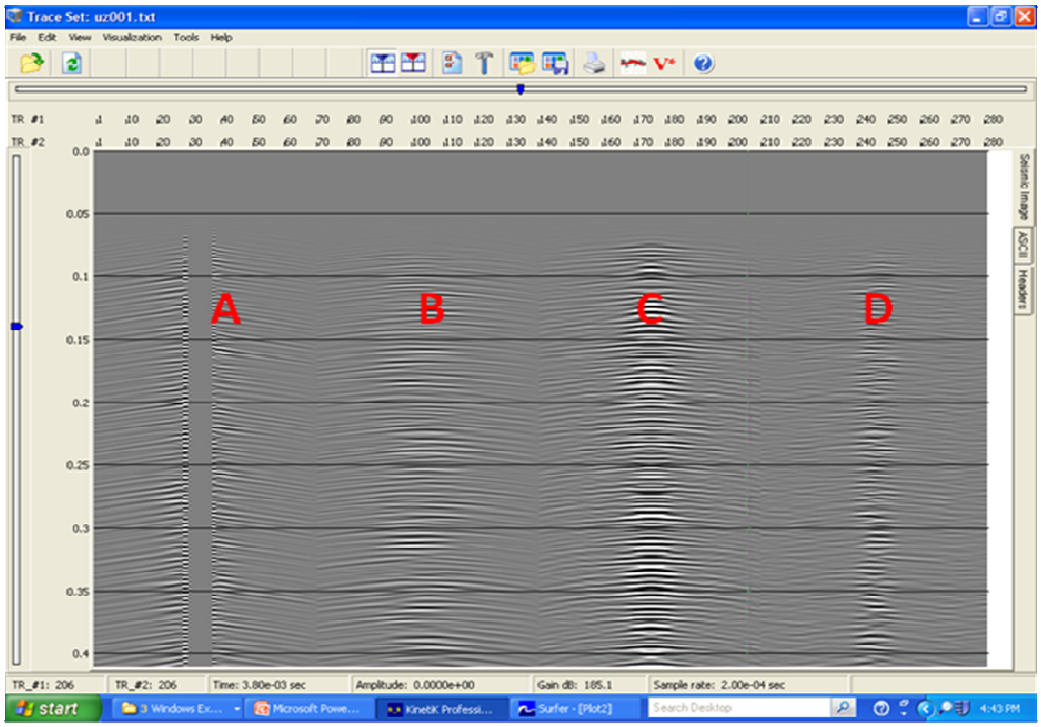


**Figure 16.** Same as on Figure 12 with first arrivals muted. Visible are durable oscillations of the resonant emission.

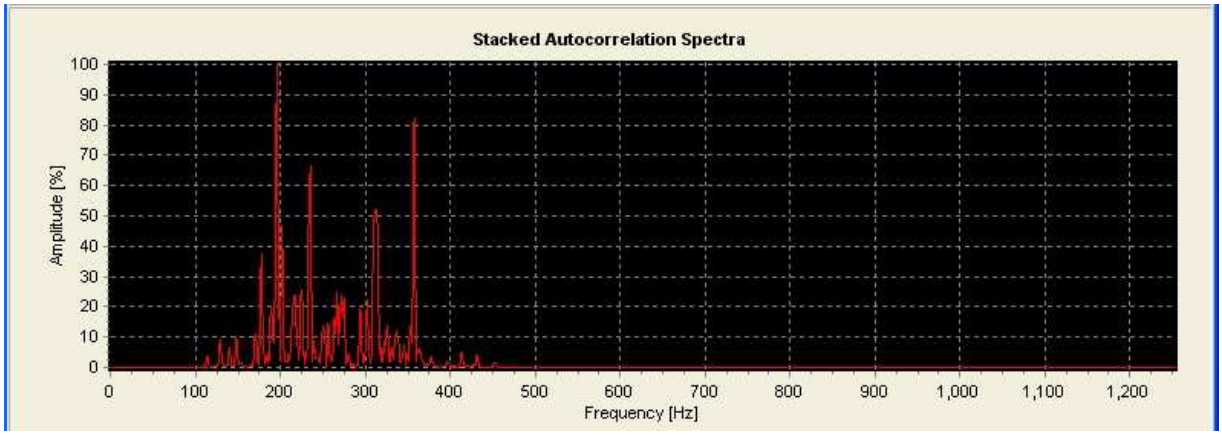


**Figure 17.** Stacked autocorrelation spectrum of the traces from Figure 16. Note similarity of peaks with those from Figure 13.

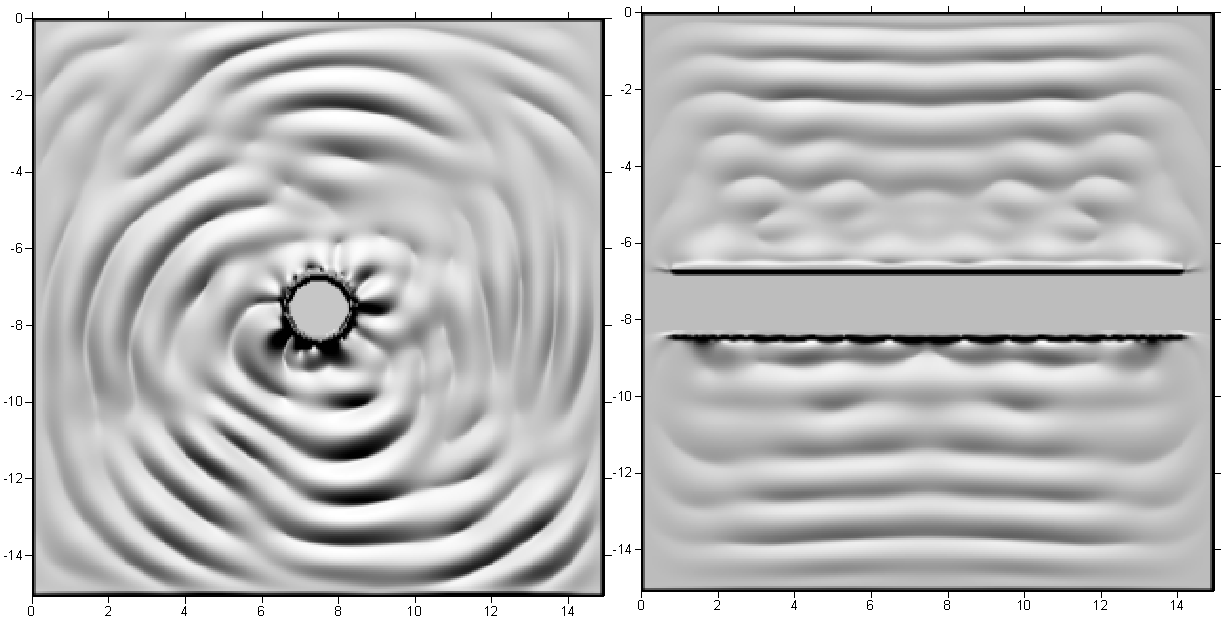


**Figure 18.** Sesmic field snapshots for the case of void and a plane incident wave at 0.2 s. Resonance emission waves propagate as quasi-spherical waves away from the cylinder (left panel) while for y=const. the waves phases are almost constant along the x axis (right panel).

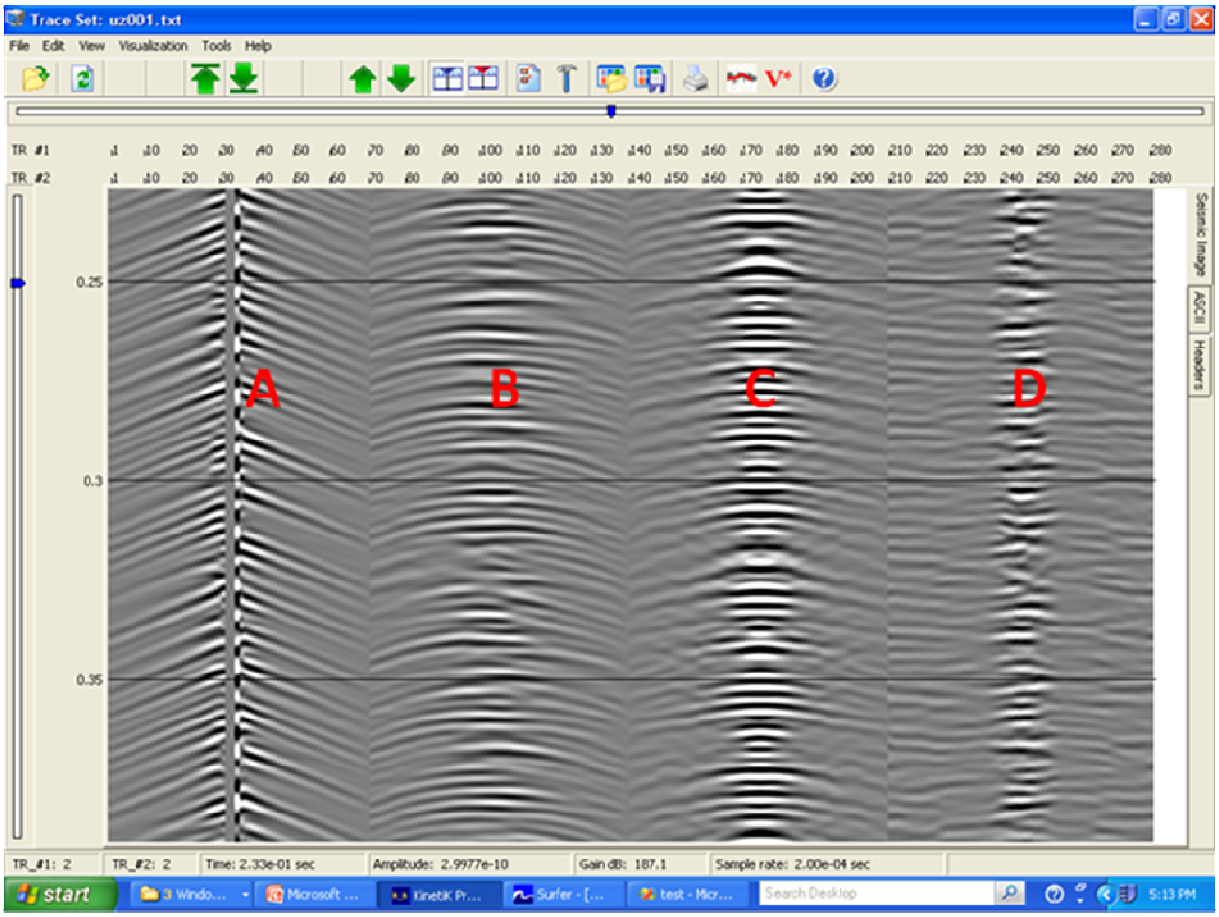


**Figure 19.** Late arrivals for traces recorded for a void cylinder with 0.5 m radius for a point-pressure source.

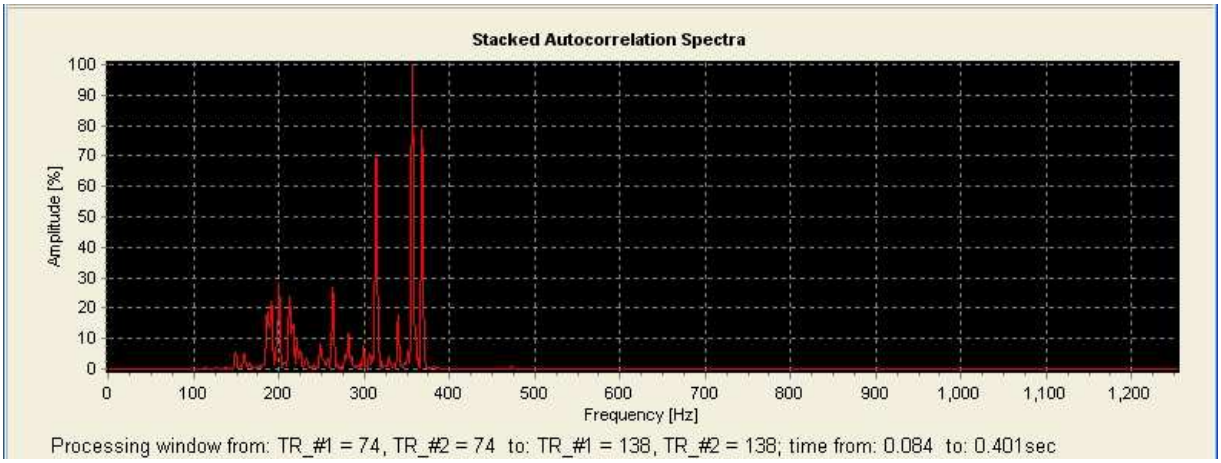


**Figure 20.** Stacked autocorrelation spectrum of the traces from Figure 18. Note the shifts towards the higher frequencies for the resonant peaks compared to those from Figure 17.

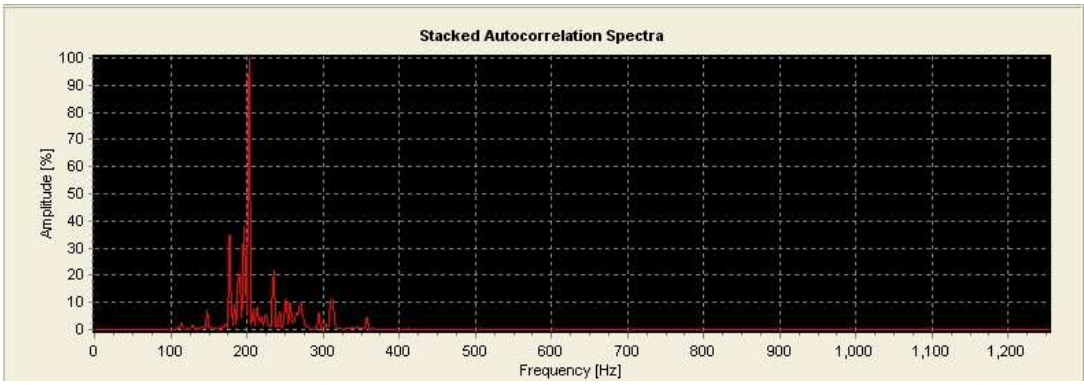


**Figure 21.** Stacked autocorrelation spectrum of the traces for a cylindrical void with 1 m radius and an incident plane p- wave.

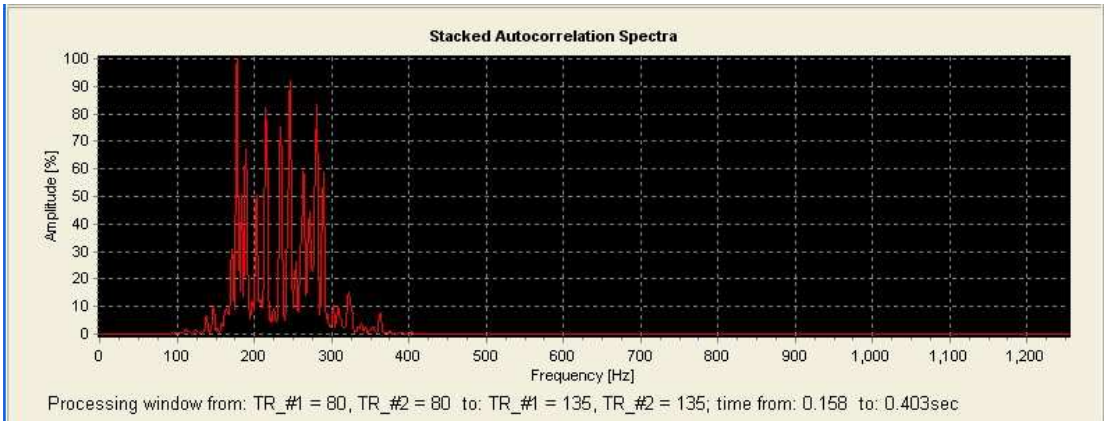


**Figure 22.** Stacked autocorrelation spectrum of the traces for a cylindrical void with 1.5 m radius and an incident plane p- wave.

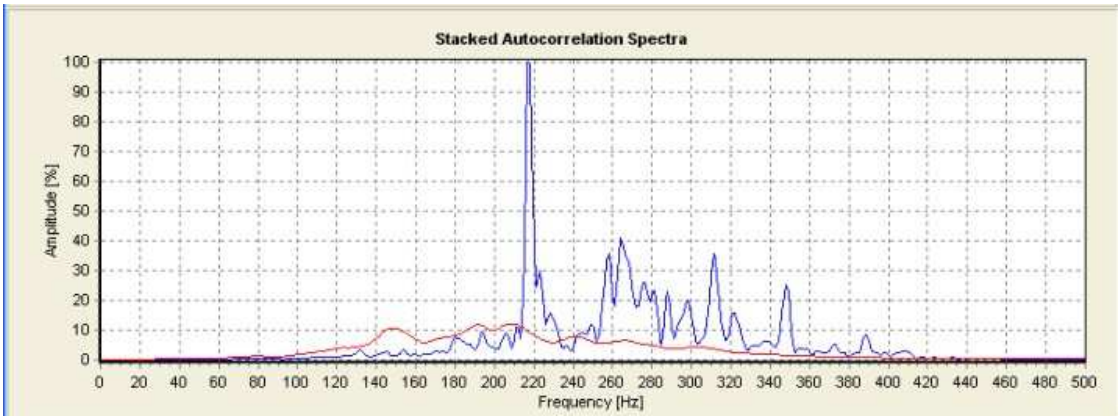


**Figure 23.** Stacked autocorrelation spectrum of the late arrival traces of the profile B for a cylindrical void with 1.0 m radius (blue line) and a purely homogeneous model (red line). This result suggests that the resonsnt peaks are not artifacts of the computation approach.

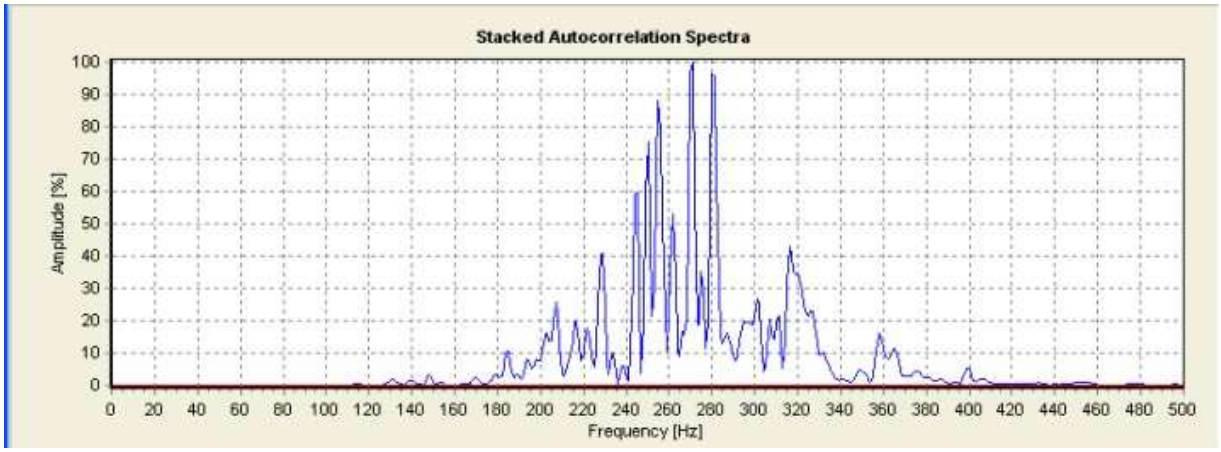


**Figure 24.** Stacked autocorrelation spectrum of the late arrival traces of the profile C for a cylindrical void with 1.0 m radius (blue line) and a purely homogeneous model (red line).

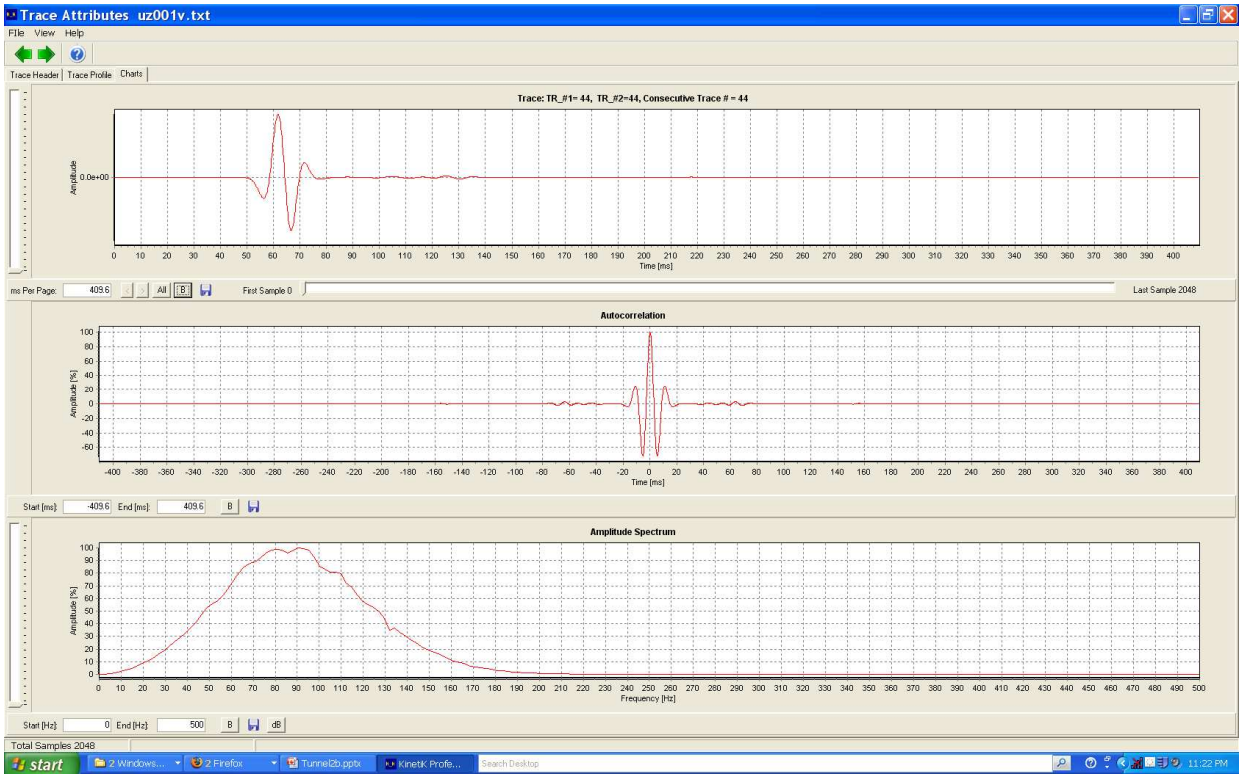


**Figure 25.** Trace record at the point source (upper panel), and its amplitude spectrum (lower panel) for lower frequency source.

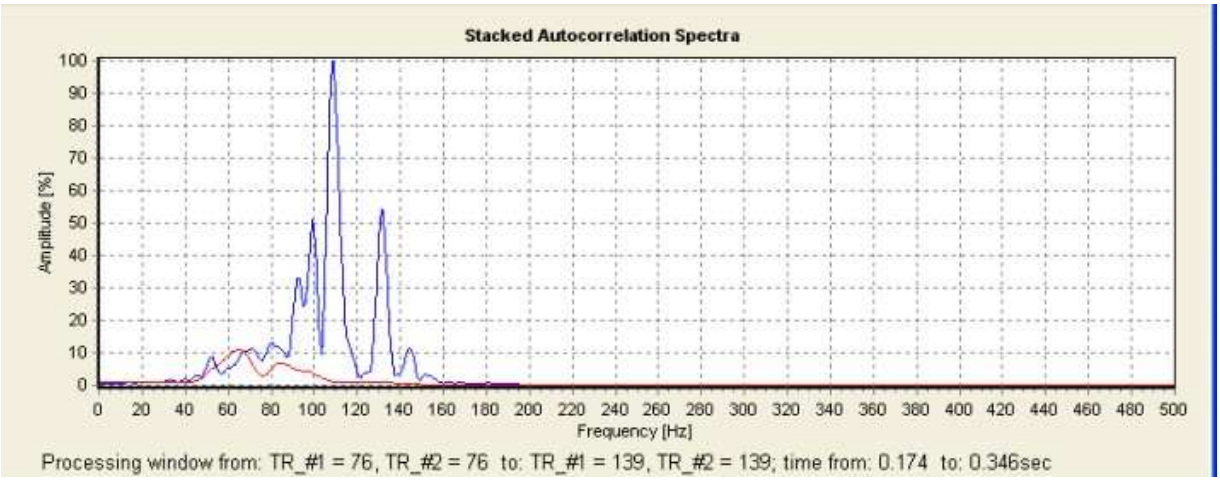


**Figure 26.** Stacked autocorrelation spectrum of the late arrival traces of the profile B for a cylindrical void with 1.0 m radius (blue line) and a purely homogeneous model (red line) at lower frequencies.

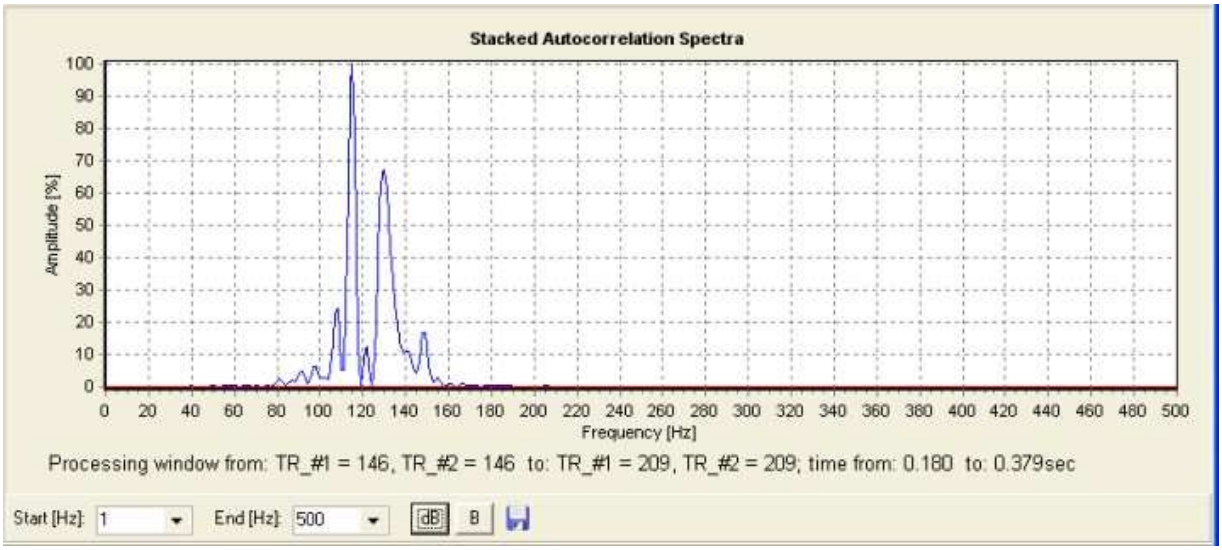


**Figure 27.** Stacked autocorrelation spectrum of the late arrival traces of the profile B for a cylindrical void with 1.0 m radius (blue line) and a purely homogeneous model (red line) at lower frequencies.

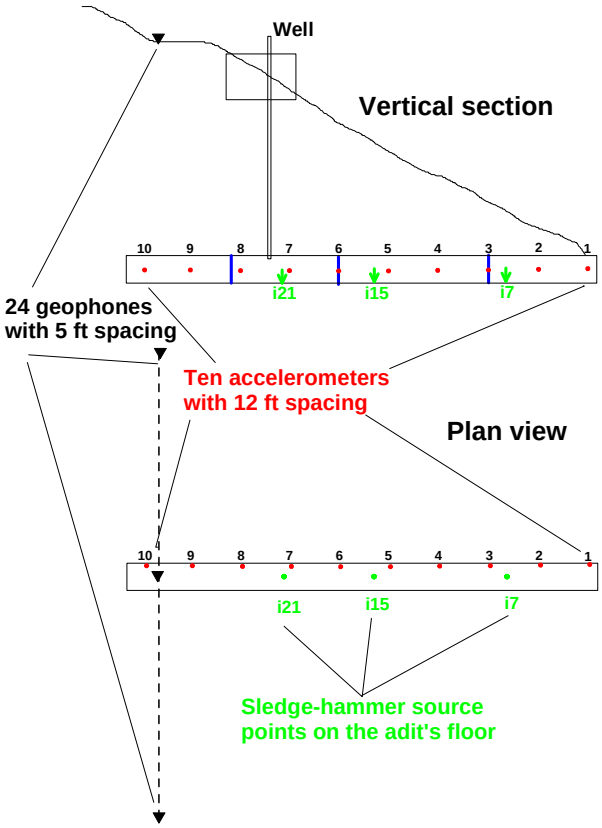


**Figure 28.** Survey Adit1 included one 24 channel geophone line with 5' spacing and 10 accelerometers in the adit with 12' spacing.

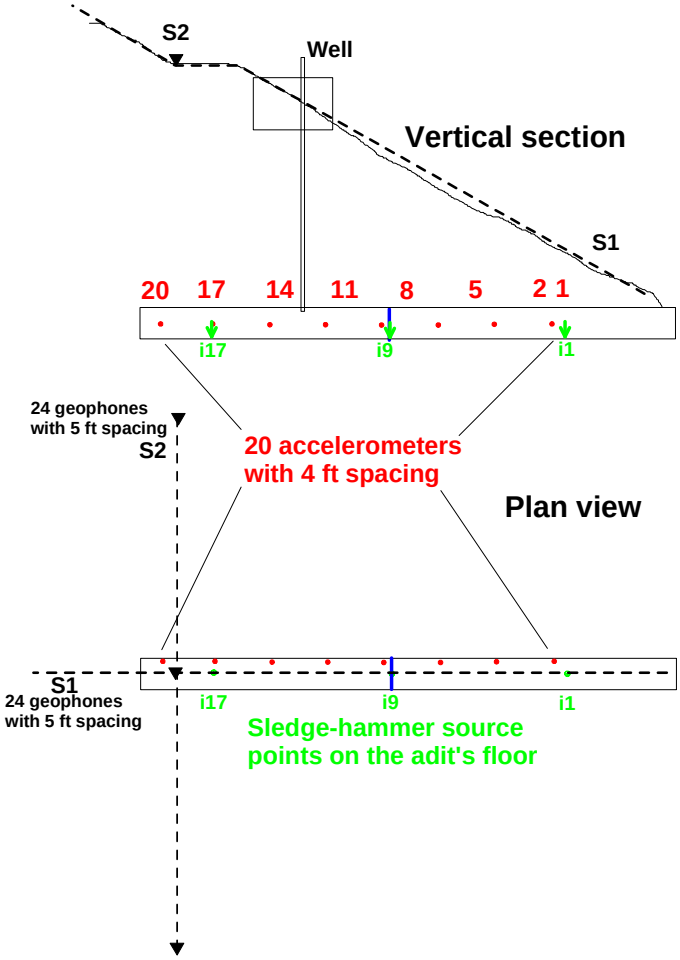


**Figure 29.** Survey Adit2 included two 24 channel geophone lines S1 and S2 with 5' spacing and 20 accelerometers in the adit with 4' spacing.

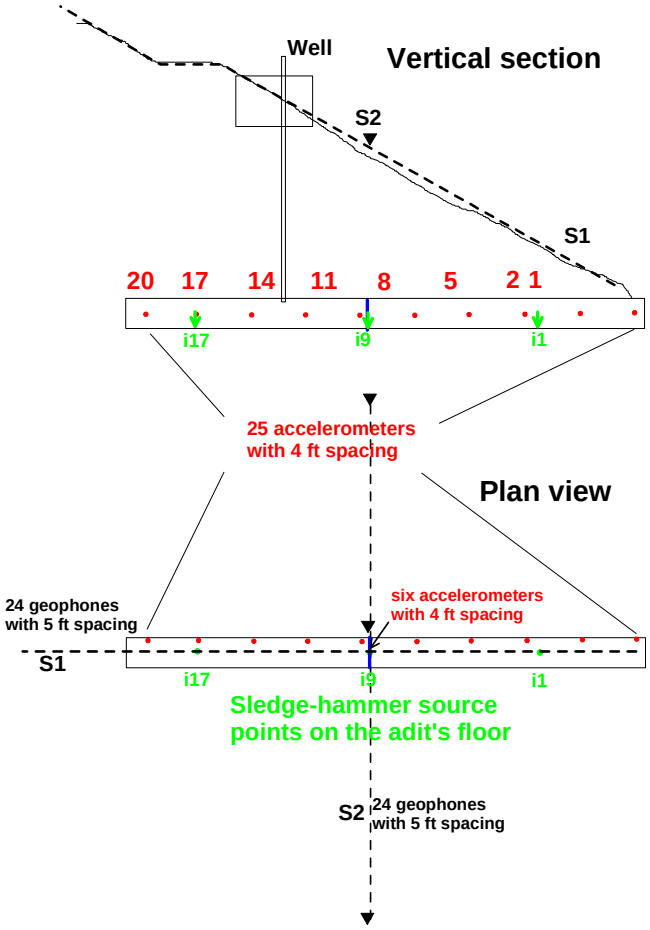


**Figure 30.** Survey Adit3 included two 24 channel geophone lines S1 and S2 with 5' spacing, 25 accelerometers in the adit with 4' spacing, and 6 accelerometers in the perimeter of the vertical section at i9 source position.

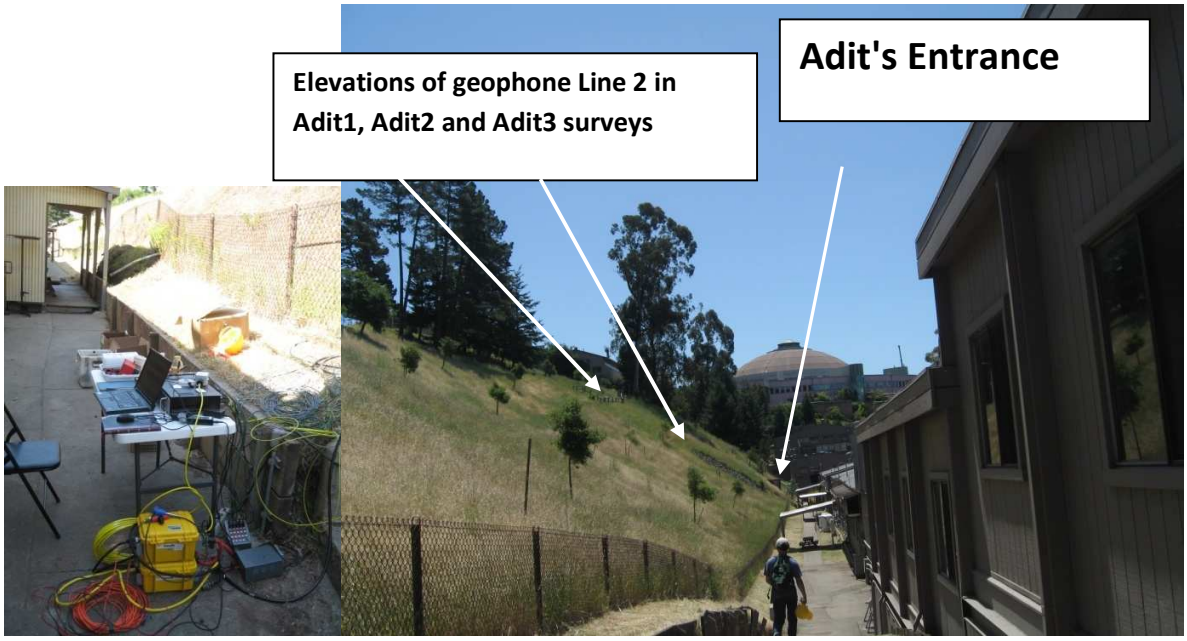


**Figure 31.** Close and far views at the field site.

**Figure 32.** Recording (left photo) and source (right photo) operations.

**Figure 33.** Accelerometer mounted on the adit's wall (left photo) and a geophone on a surface line (right photo) .

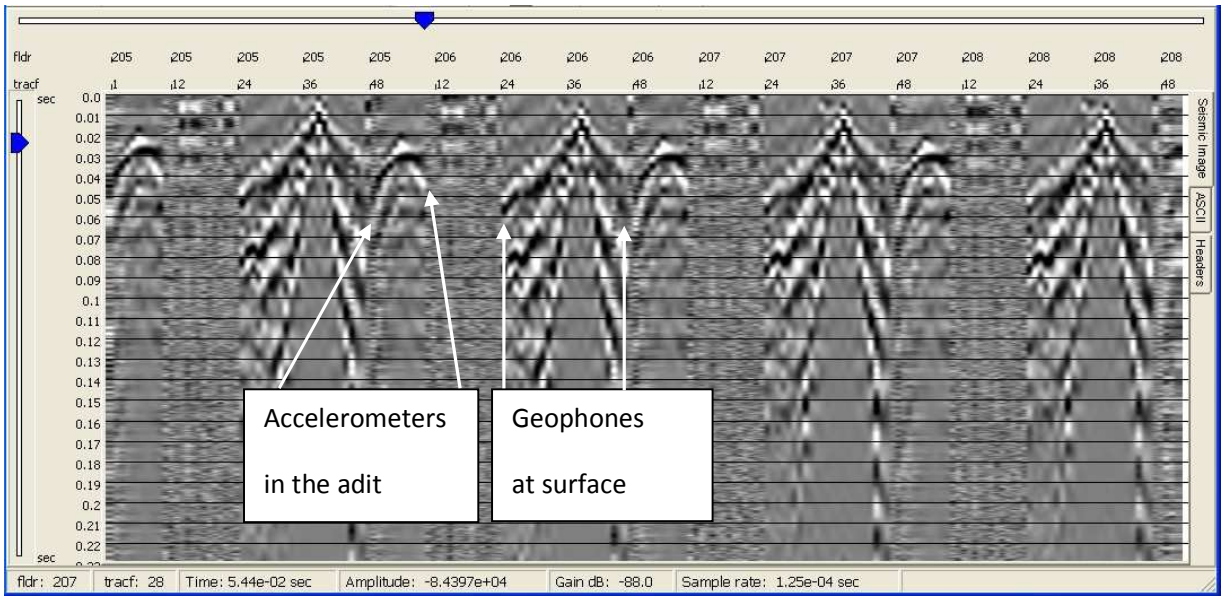


**Figure 34.** Data from repeated surface shots recorded during Adit1 survey.

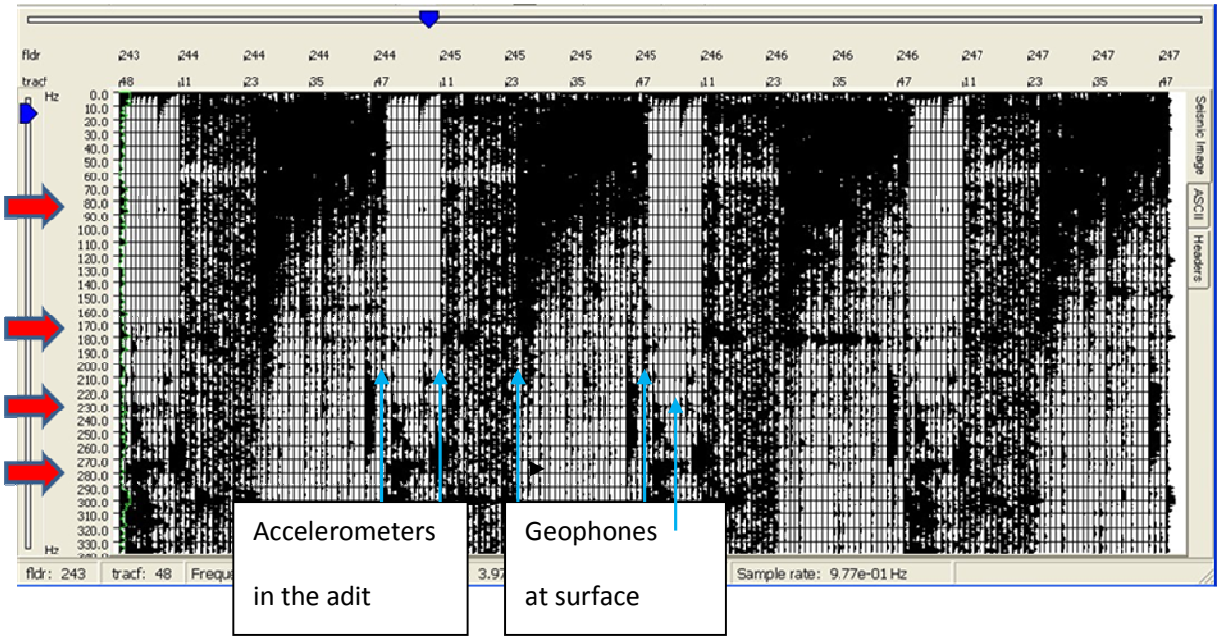


**Figure 35.** Spectrogram of repeated shots in i15 (Adit1 survey). Red arrows indicate frequency peaks at 86 Hz, 175 Hz, 235 Hz, and 275 Hz.

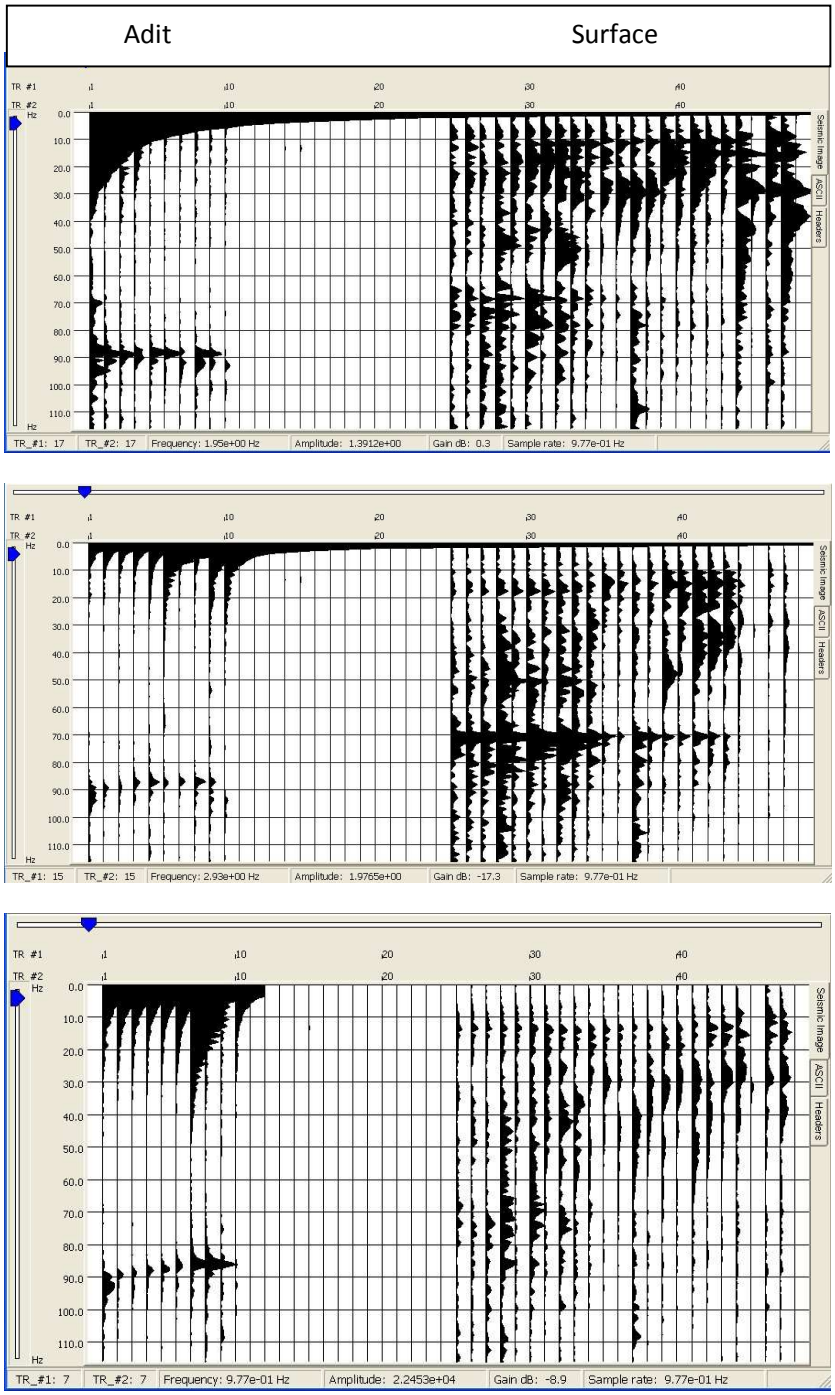


**Figure 36.** Spectrograms for shots in the adit (Adit1 survey). Sources at i7 (upper panel), i15 middle panel and i21 (lower panel). Note the resonance at 86 Hz.

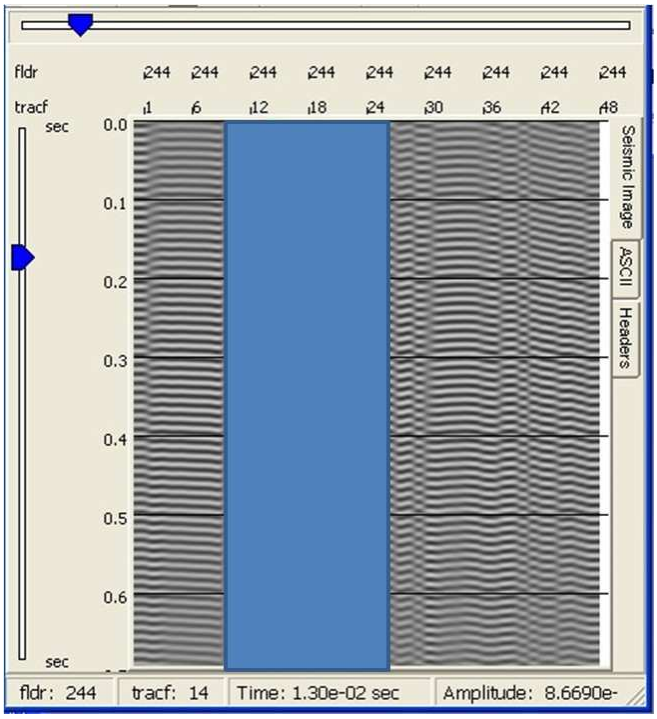


**Figure 37.** Adit (i15) hammer shot (Adit1 data). Traces 25-48-24 belong to geophone profile. Traces 1-10 are accelerometers attached to the south adit's wall with 12 ft spacing. Traces are band-pass filtered in 85-90Hz interval, and exhibit approximately hyperbolic shape indicating that the waves are radiated by the adit.

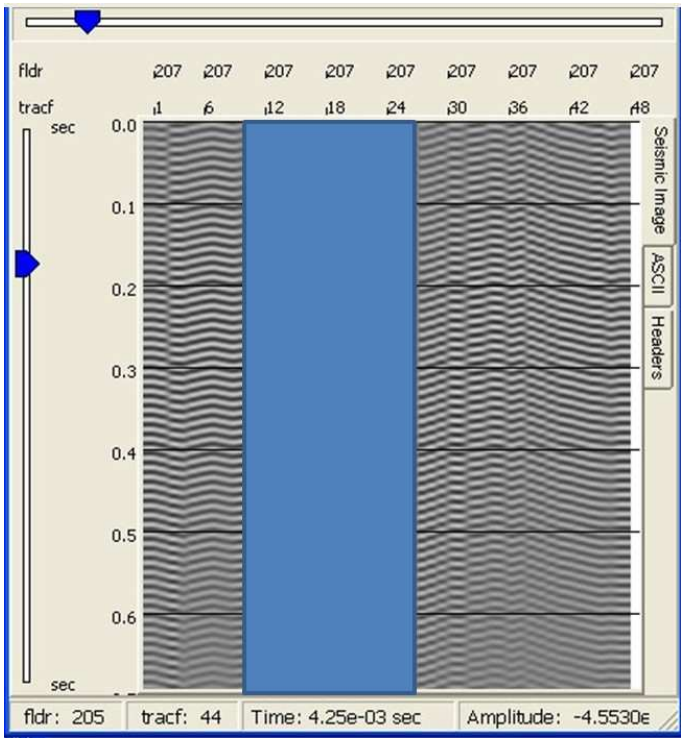


**Figure 38.** Same as on Figure 37 for the i21 shot.

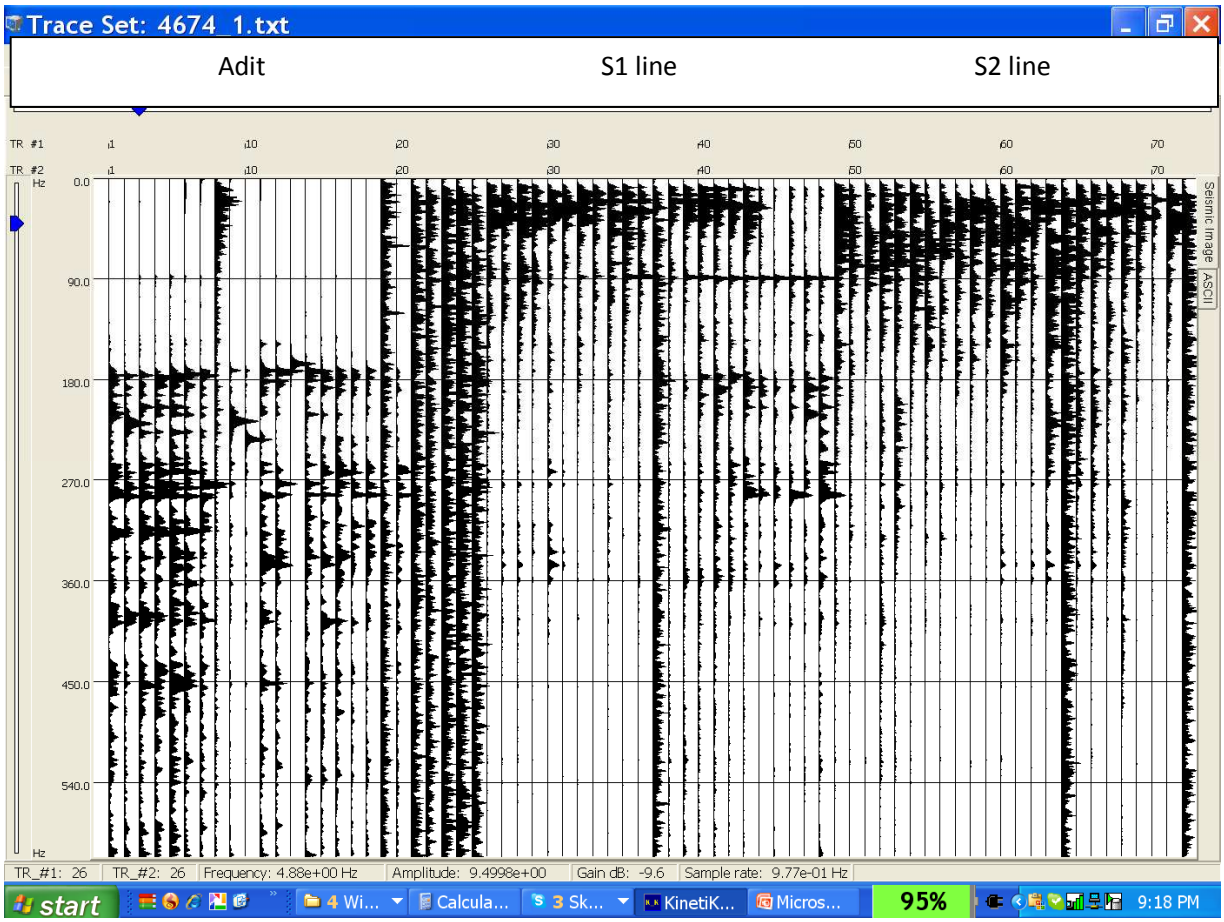


**Figure 39.** Spectrogram for i9 shot (Adit2 survey). Note the 89 Hz peak at S1 (uphill) line.

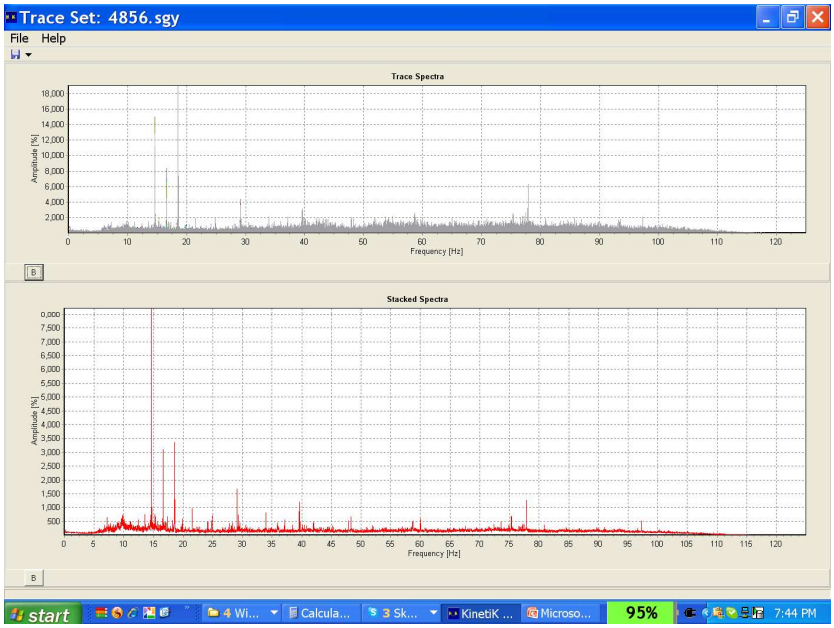


**Figure 40**. Average noise spectra for geophones (Adit2 survey).

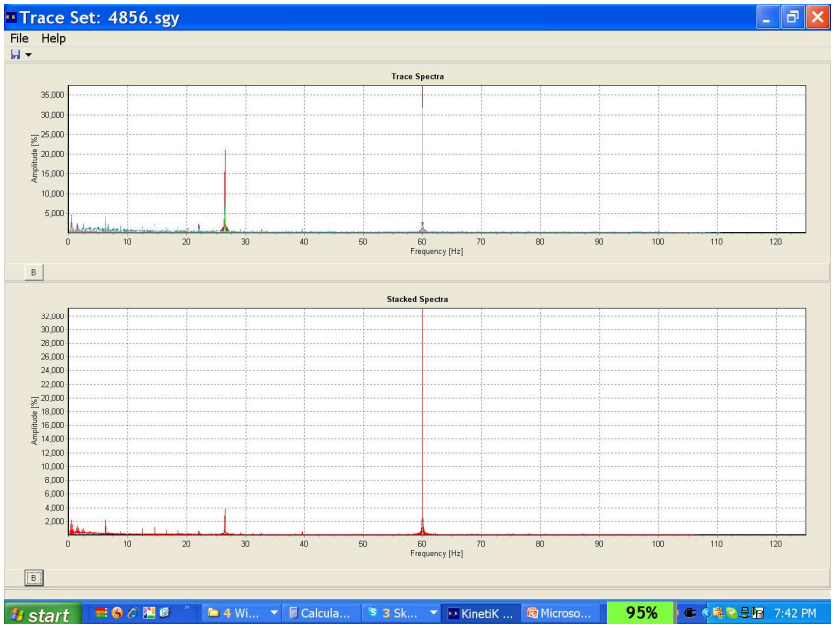


**Figure 41**. Average noise spectra for accelerometers (Adit2 survey).

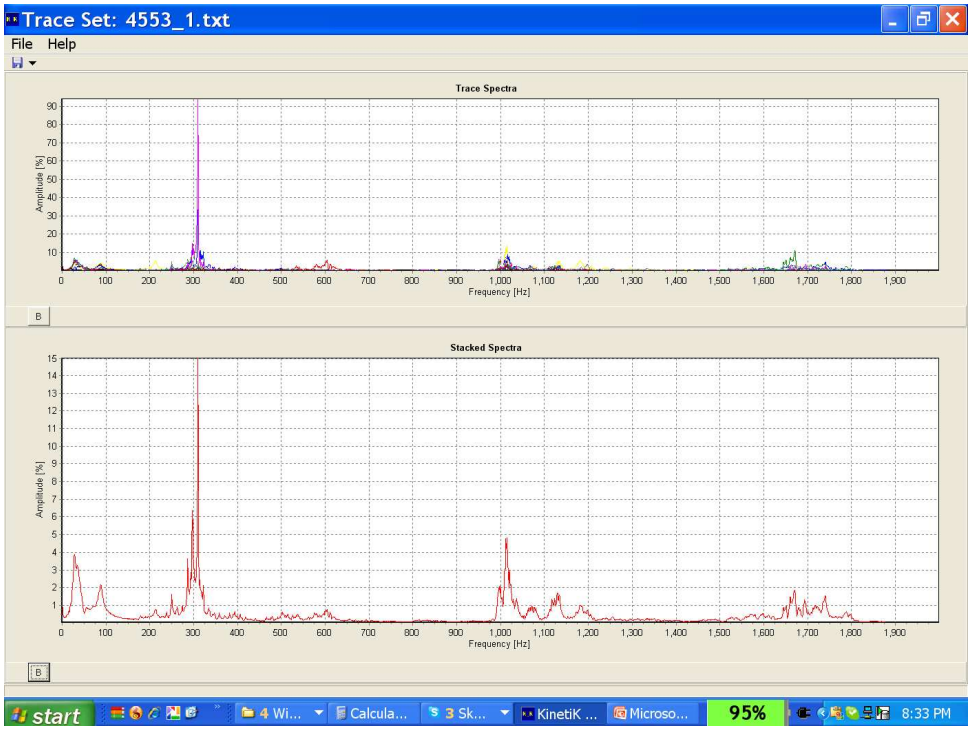


**Figure 42**. Average spectra of late phases in the adit after a sledge hammer hit of the concrete base near wellhead (Adit2 survey). Note a resonant peak at 90 Hz.

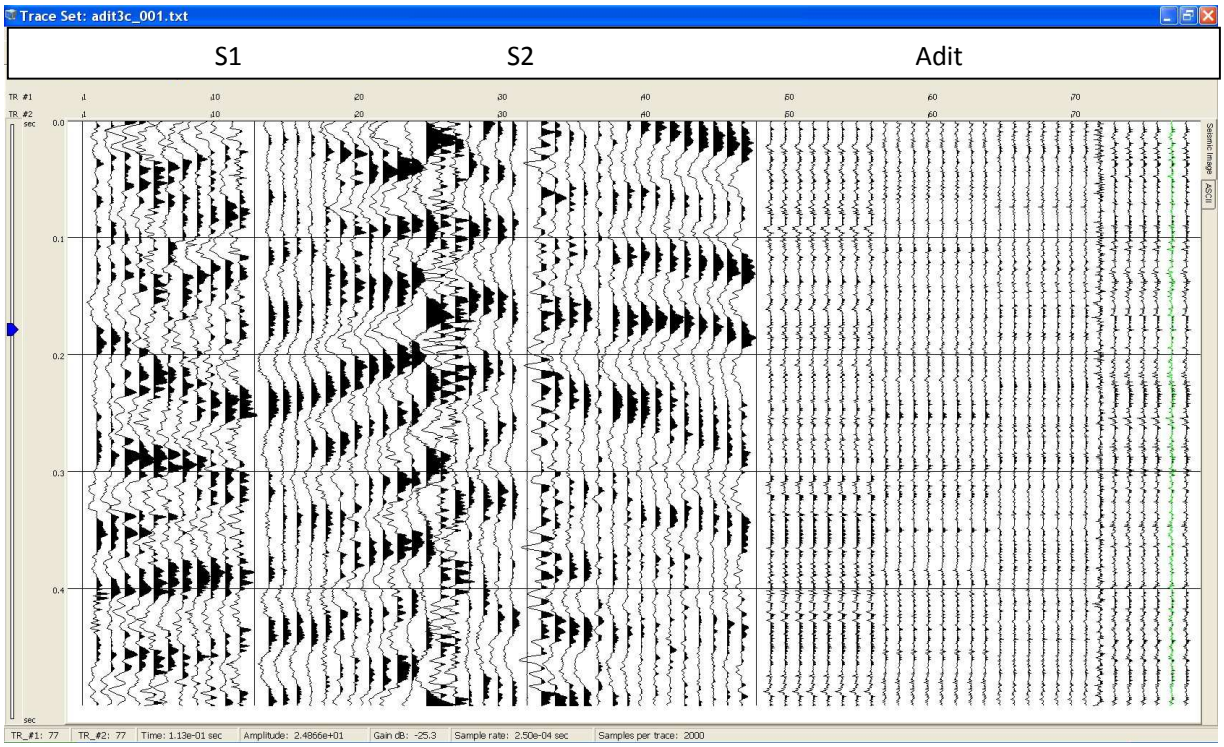


**Figure 43.** Ambient noise records (Adit3 data).

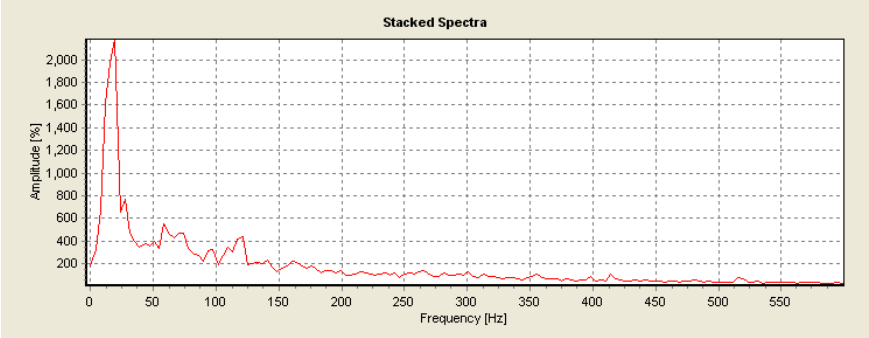


**Figure 44.** Stacked amplitude spectra of ambient noise for the geophone data (Adit3 data).

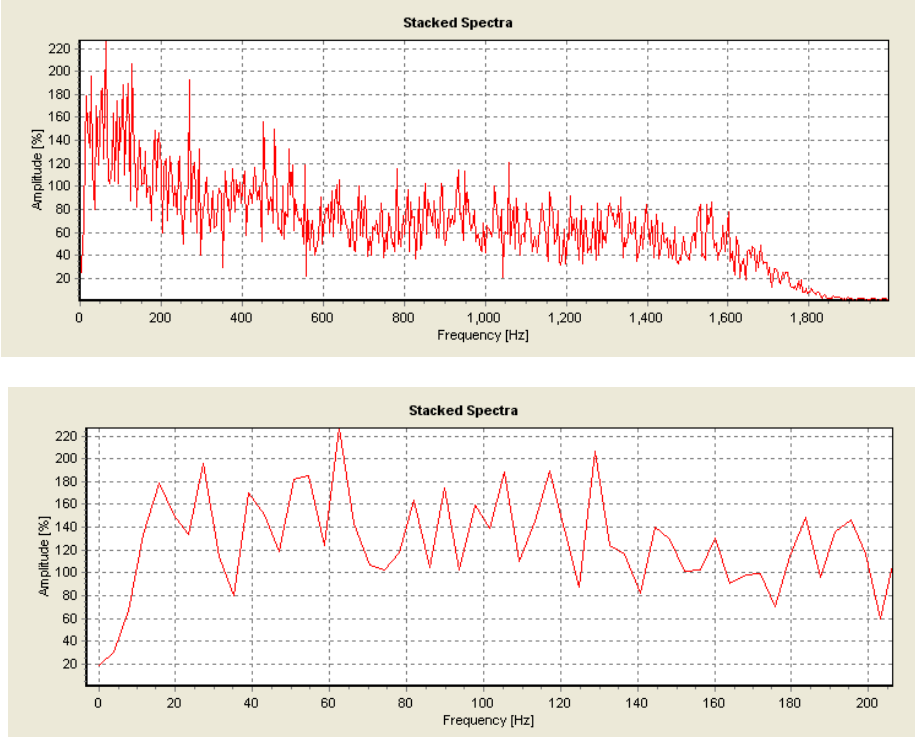


**Figure 45.** Upper panel - stacked amplitude spectra of ambient noise for the accelerometer data (Adit3 data). Lower panel - detail view of lower frequencies part .

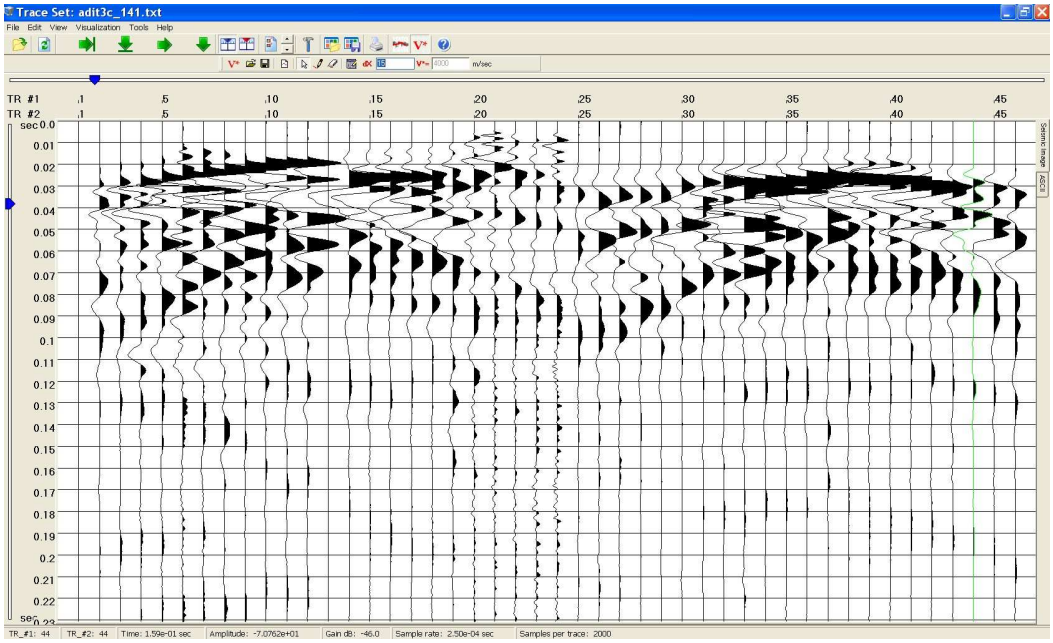


**Figure 46.** Geophone traces from i9 hammer shot. Traces 1-24 belong to geophone profile S1 (Sensor 1 is uppermost on top of the hill). Traces 25-48 belong to orthogonal (North-South) geophone profile S2 . Per trace normalization.

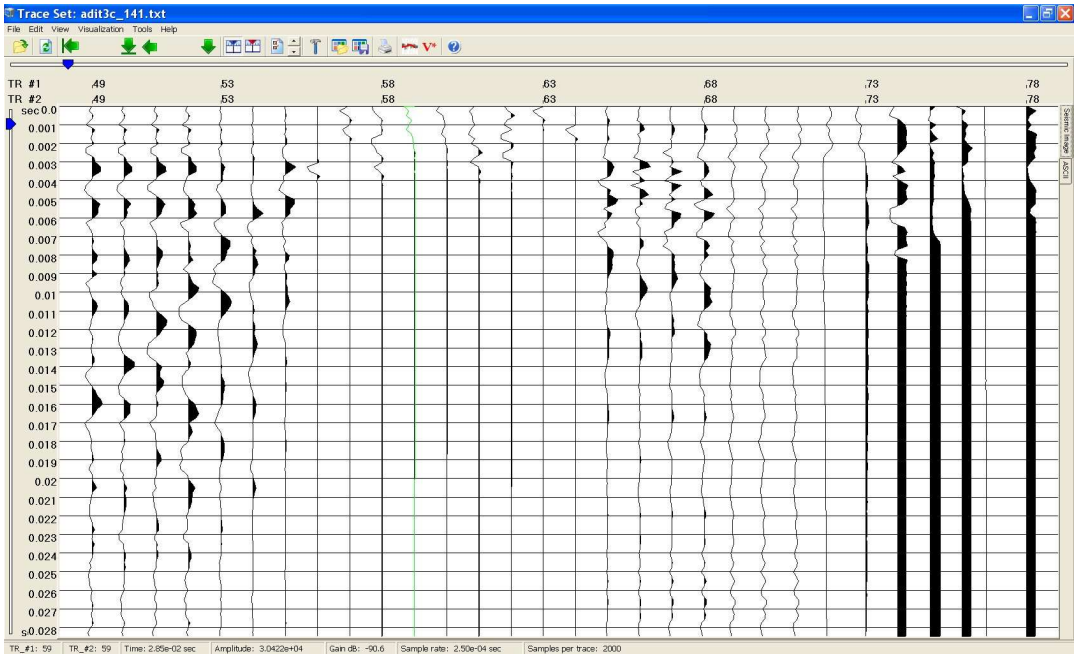


**Figure 47.** Adit (i9) hammer shot (Adit3 data). Per trace normalized accelerometer traces.

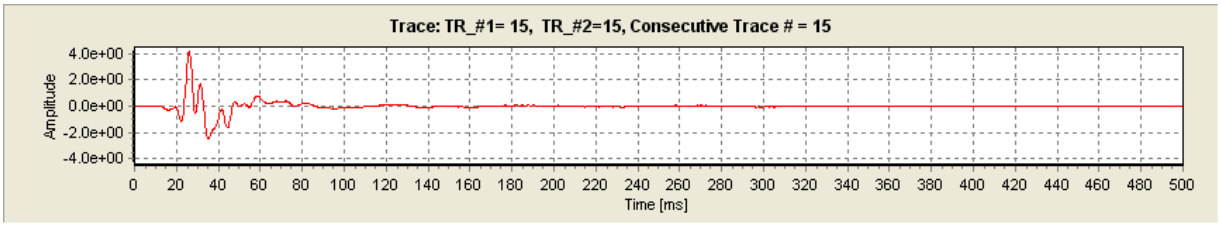


**Figure 48.** Adit (i9) hammer shot (Adit3 data) recorded at geophone #15 (middle of S1 profile).

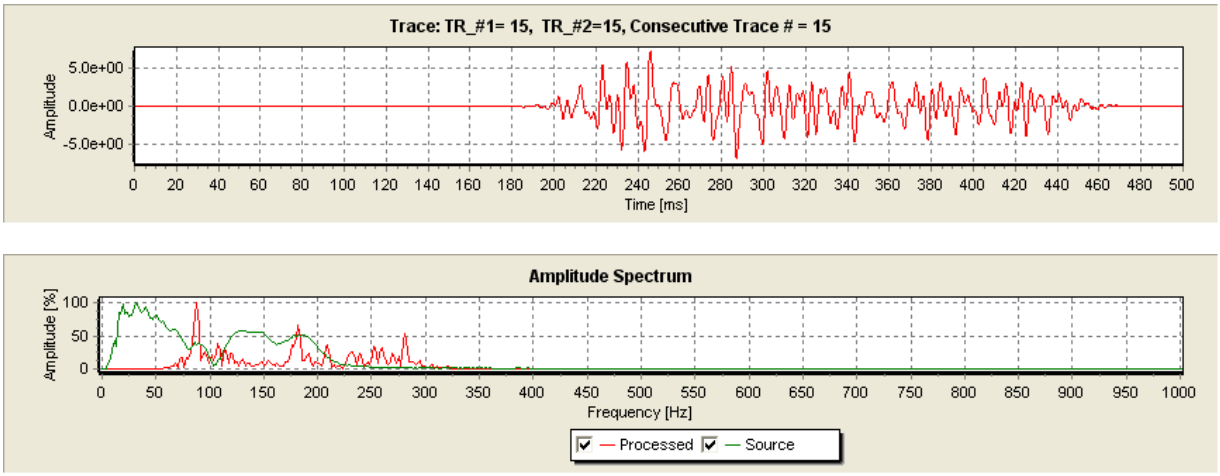


**Figure 49.** Adit (A9) hammer shot (Adit3 data) recorded at geophone #15 (Figure 48 ). Upper panel - gated (0.2 - 0.45 ms) and bandpass (70 - 400 Hz) filtered trace. Bottom panel - amplitude spectra of the trace above (red) and the raw trace (green). Clearly visible is 89 Hz resonant peak.

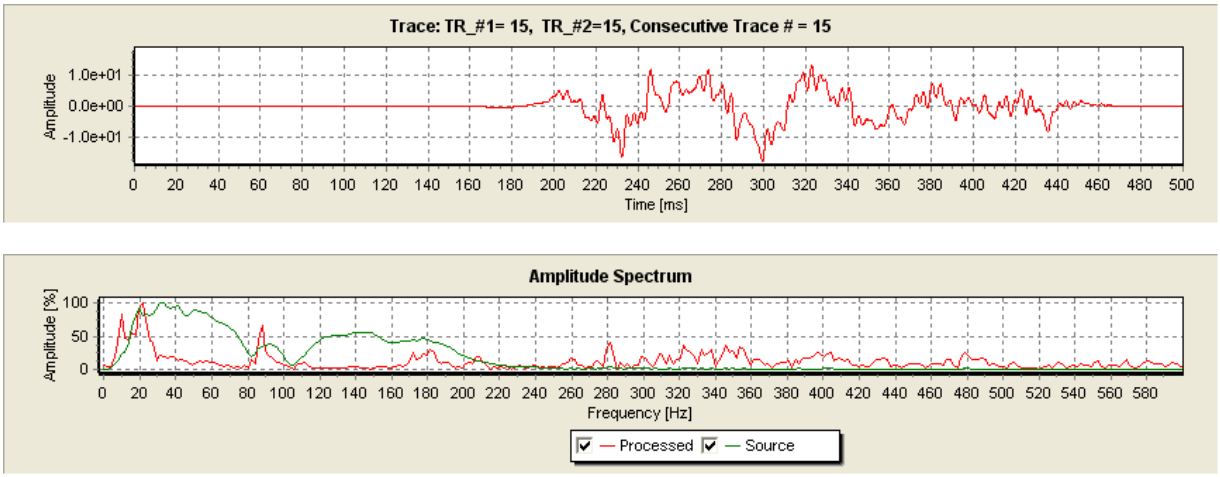


**Figure 50.** Adit (A9) hammer shot (Adit3 data) recorded at geophone #15. Upper panel - gated (0.2 - 0.45 ms) and bandpass (15 - 400 Hz) filtered trace. Bottom panel - amplitude spectra of the trace above (red) and the raw trace (green).

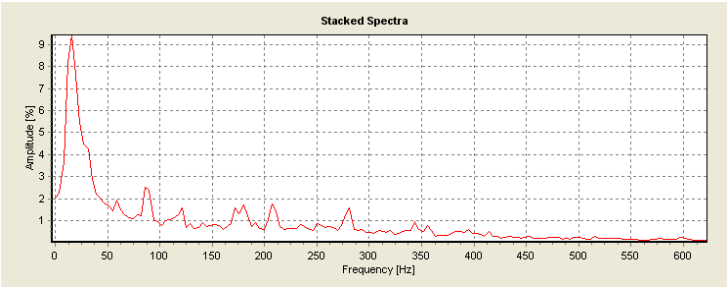


**Figure 51.** Stacked geophone spectra for adit (i9) hammer shot (Adit3 data).

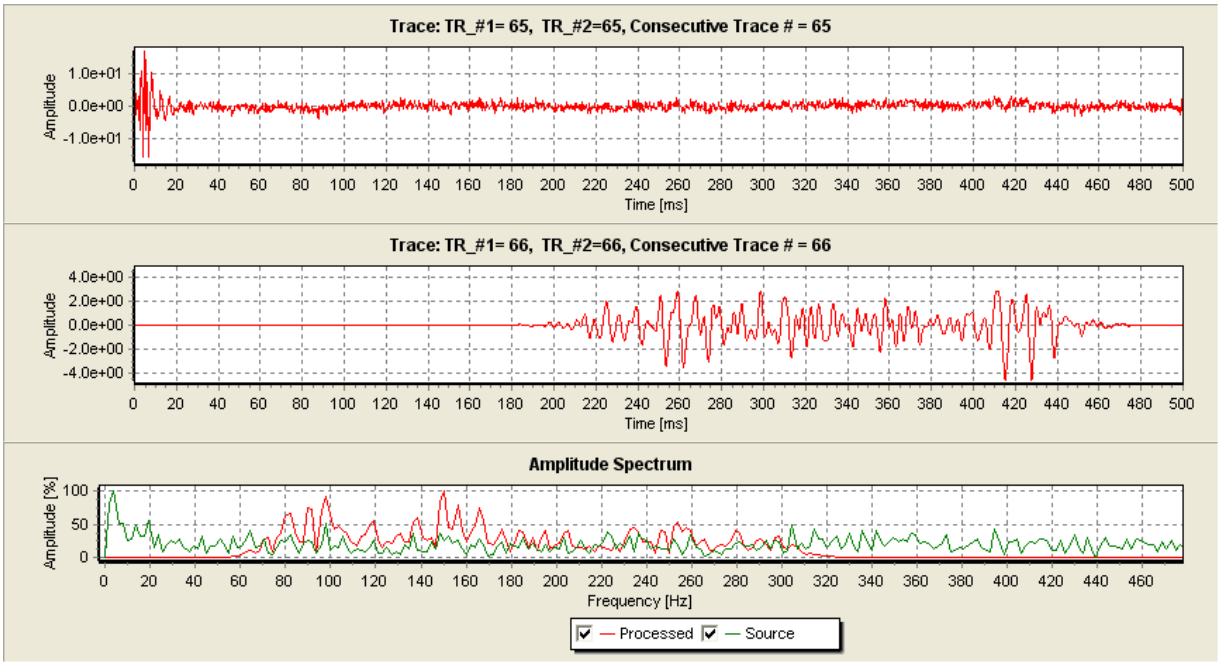


**Figure 52.** Typical accelerometer record (upper panel). After gating (middle panel). Amplitude spectra of the raw trace (green color) and gated ( also bandpassed for 70 - 400 Hz) late phases (red color).

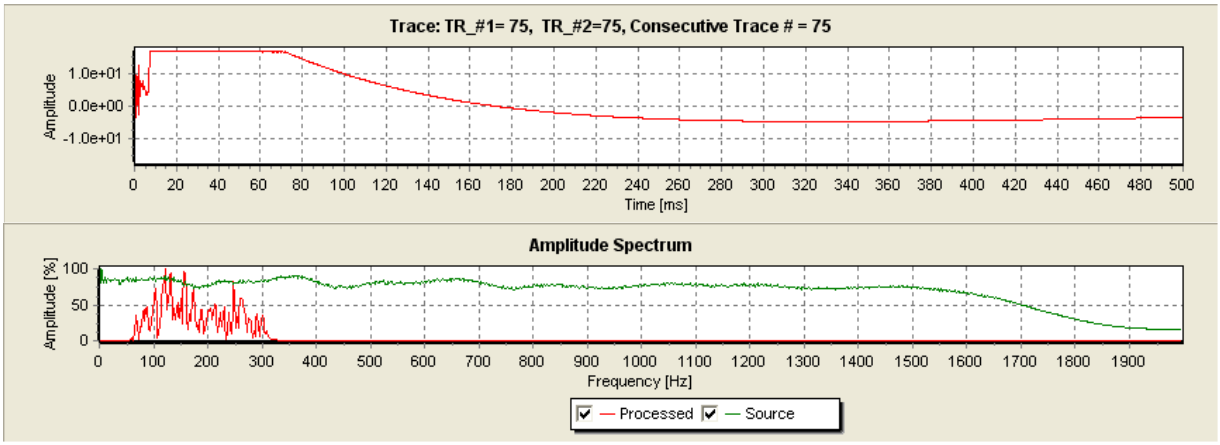


**Figure 53.** Example of dynamic clipping for accelerometer record (upper panel). Amplitude spectra of the raw trace (green color) and gated late phases (red color).

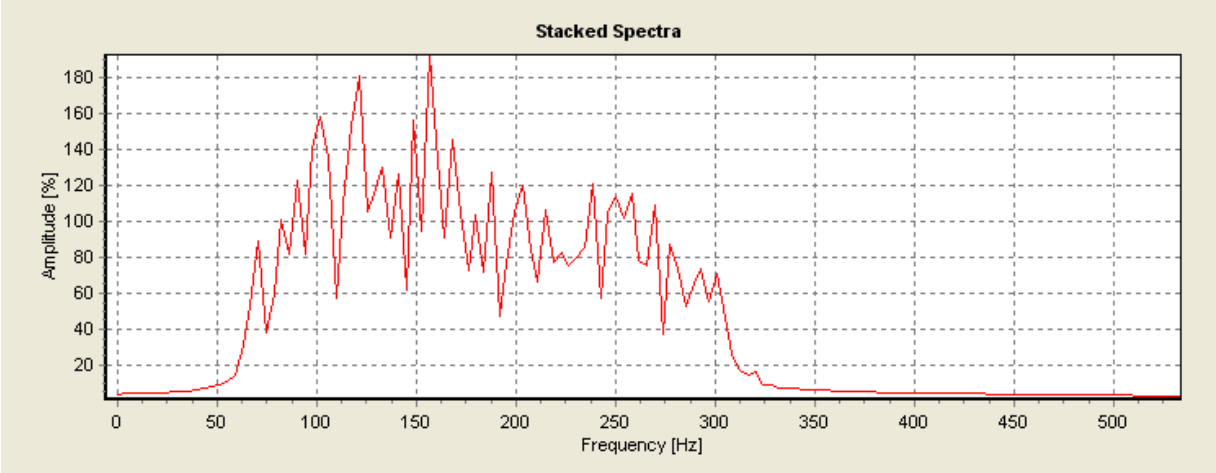


**Figure 54.** Stacked accelerometer spectra for adit (i9) hammer shot (Adit3 data). Bandpass (60 - 300 Hz) filtered.

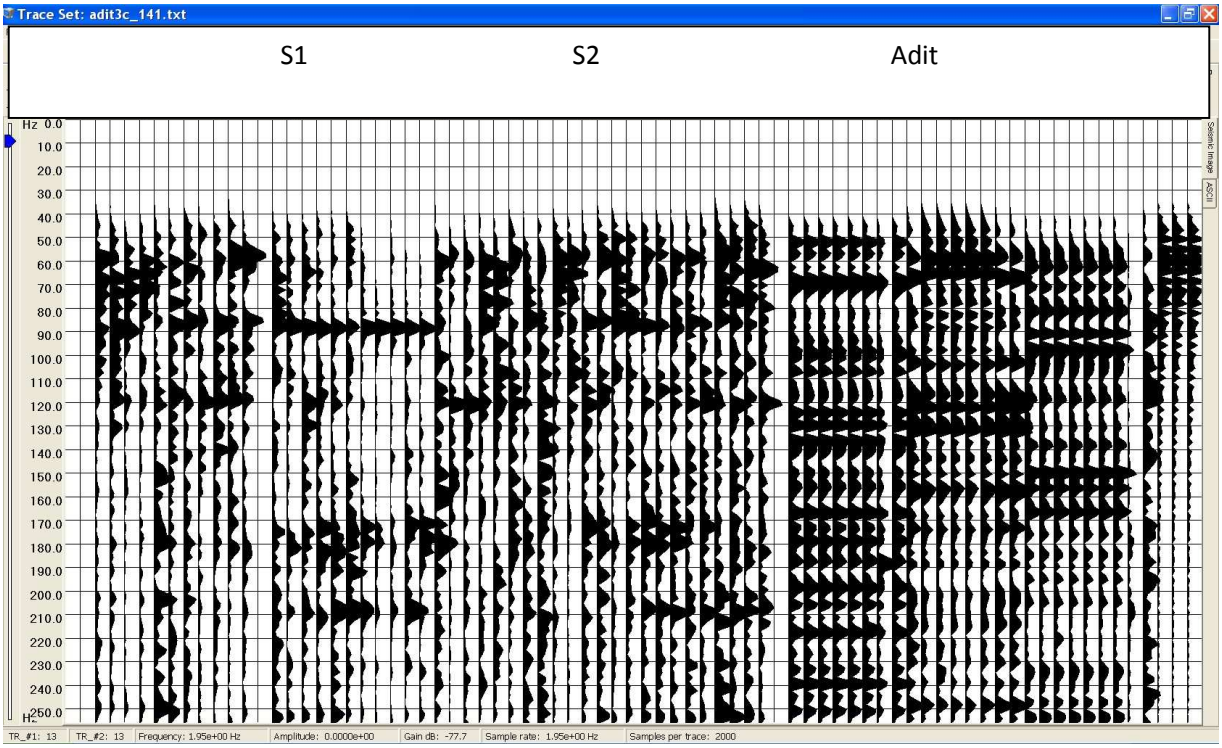


**Figure 55.** Spectrogram for the adit (i9) hammer shot (Adit3 data). Bandpass (50 - 300 Hz) filtered.

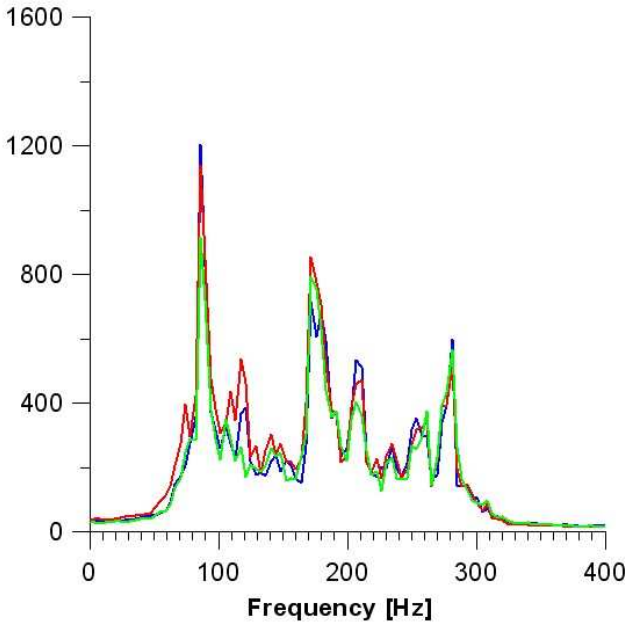


**Figure 56.** Repeatability of geophone responses for three series of shots in i9 executed with one hour interval.

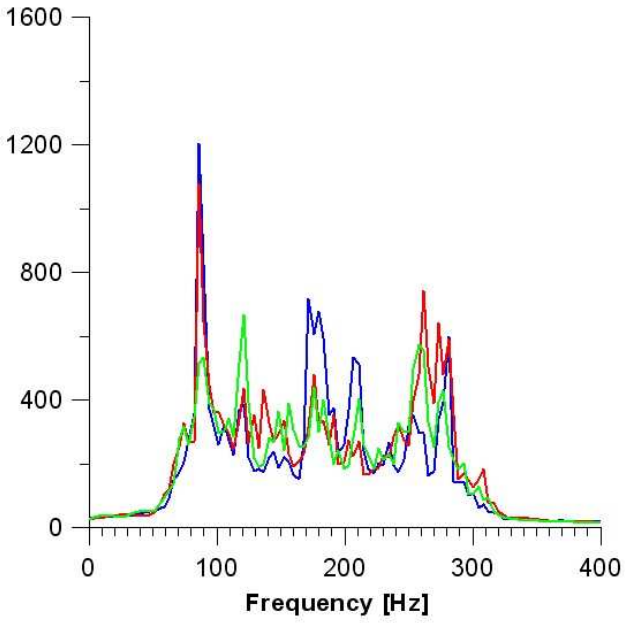


**Figure 57.** Stacked amplitude spectra of geophone records for i1 (red color) , i9 (blue color) and i17 (green color) shot points.

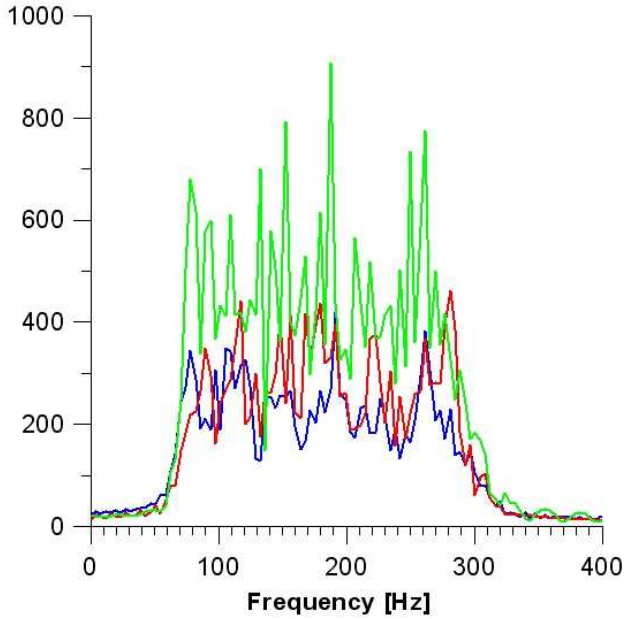


**Figure 58.** Stacked amplitude spectra of accelerometer records (radial component) for i1 (red color) , i9 (blue color) and i17 (green color) shot points.

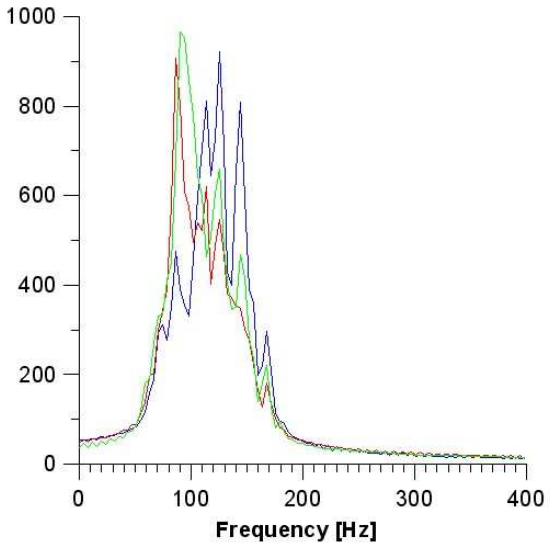


**Figure 59.** Stacked amplitude spectra of accelerometer records (radial component) for vertical surface hits in points P1 (blue color) , P2 (red color) , and P3 (green color).

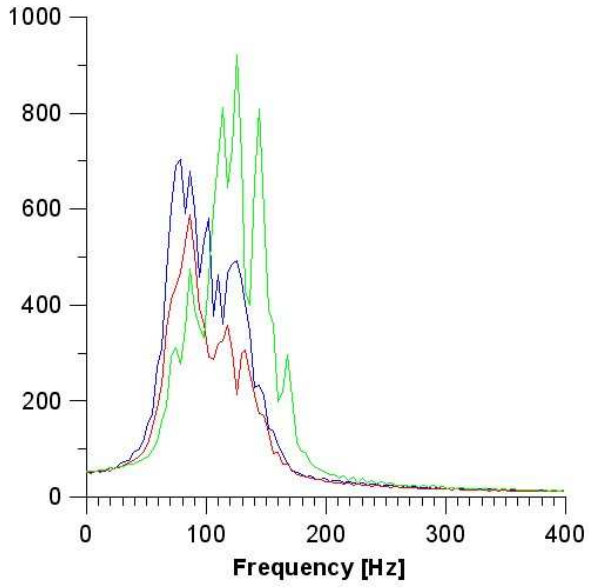


**Figure 60.** Stacked amplitude spectra of geophone records for vertical surface hits in points P1 (blue color) , P2 (red color) , and P3 (green color).

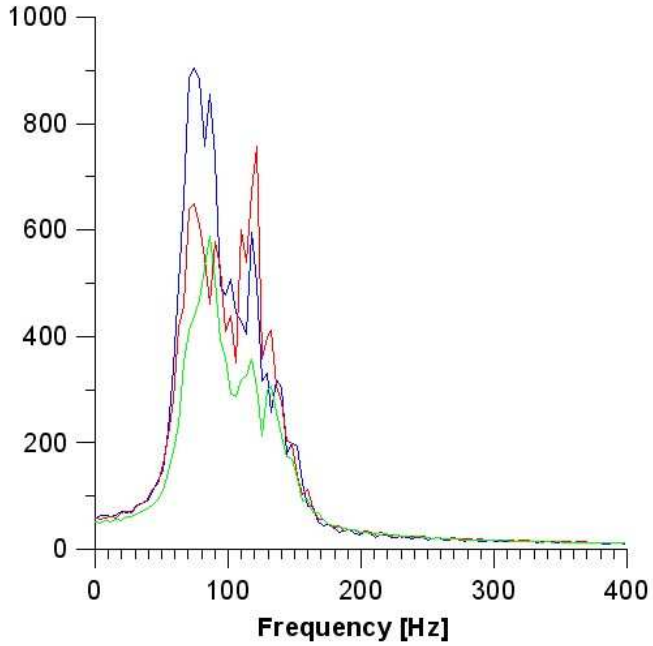


**Figure 61.** Stacked amplitude spectra of geophone records for hits in P1: North-South (blue color) , West-East(red color) , and Vertical (green color).

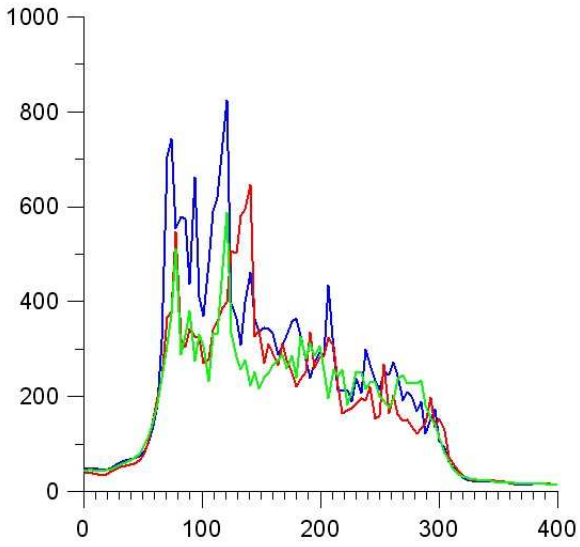


**Figure 62.** Stacked amplitude spectra of accelerometer records (radial component) for West-East surface hits in points P1 (blue color) , P2 (red color), and P3 (green color).

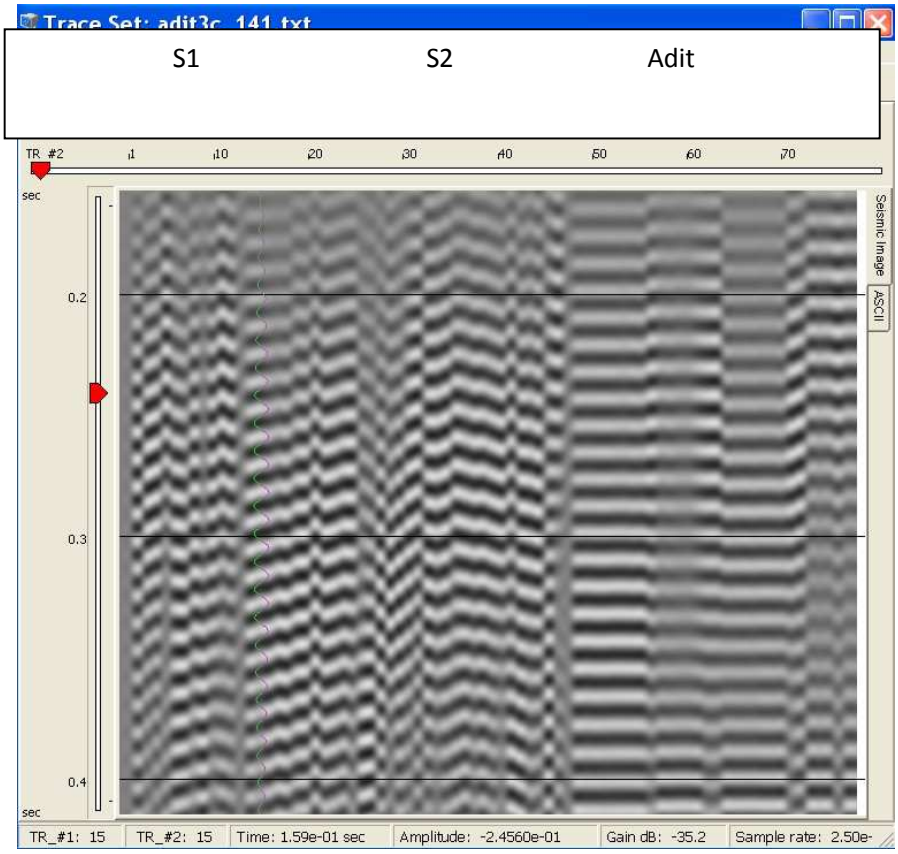


**Figure 63.** Adit (i9) hammer shot (Adit3 data). Traces 1-24 belong to geophone profile 1 (Sensor 1 is uppermost on top of the hill). Traces 25-48 belong to orthogonal (North-South) geophone profile 2 . Traces 49-73 are accelerometers attached to the south adit's wall with 4 ft spacing. Traces are band-pass filtered in 85-90Hz interval. S2 traces exhibit approximately hyperbolic shape indicating that the waves are radiated by the adit.

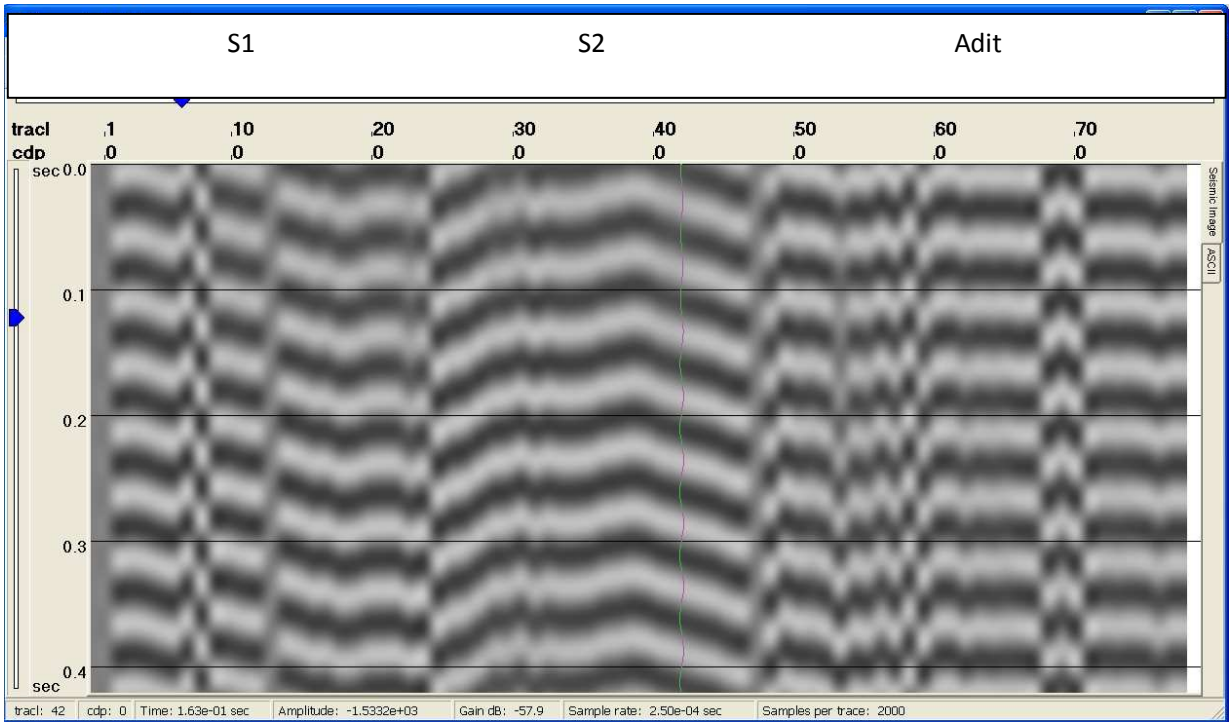


**Figure 64.** Same as on Figure 63, for 21 Hz resonance frequency.

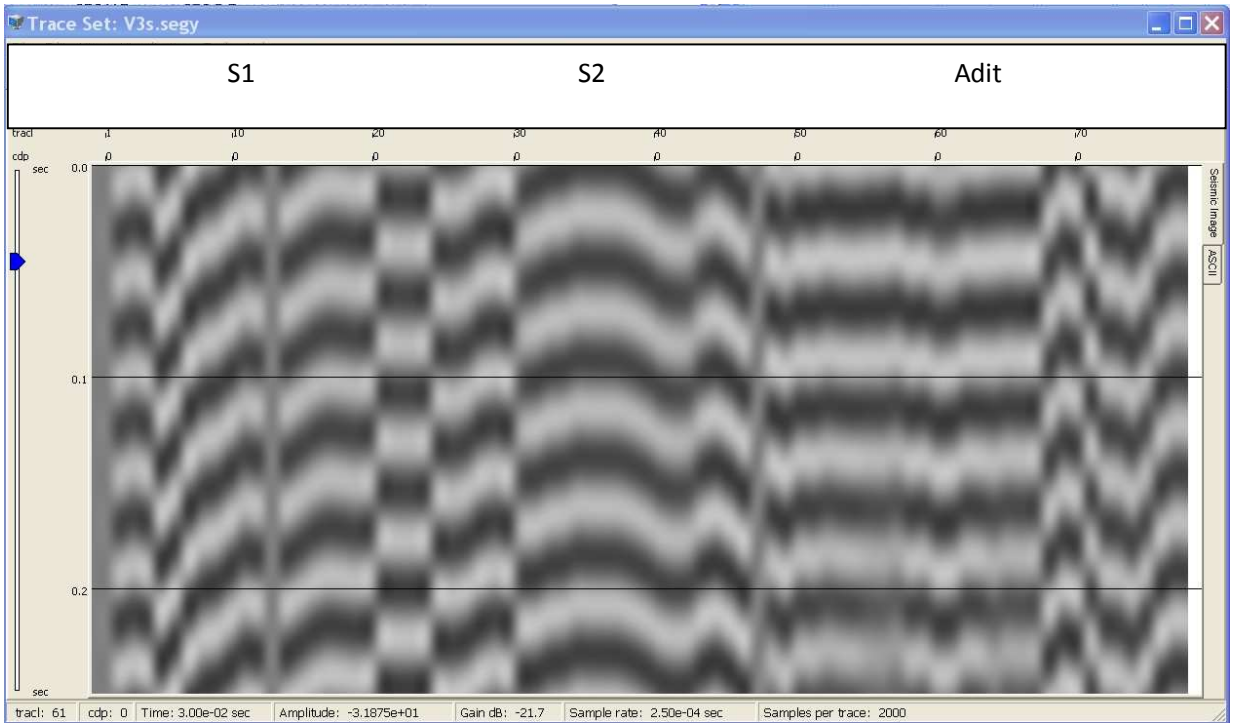


**Figure 65.** Same as on Figure 65, for a surface vertical shot at P3 source location.

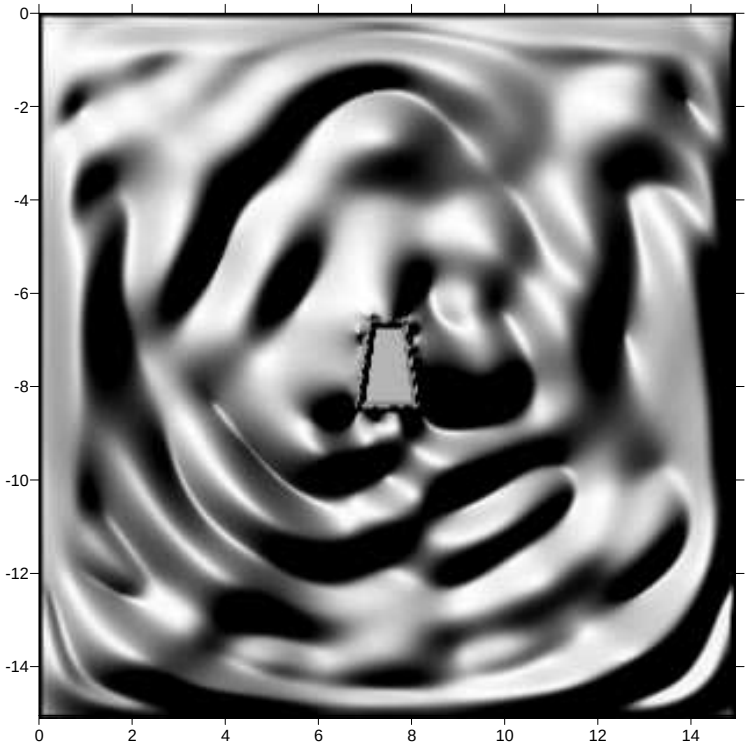


**Figure 66.** Wavefield x=7.5 m snapshot at 0.2 s for adit FD model.

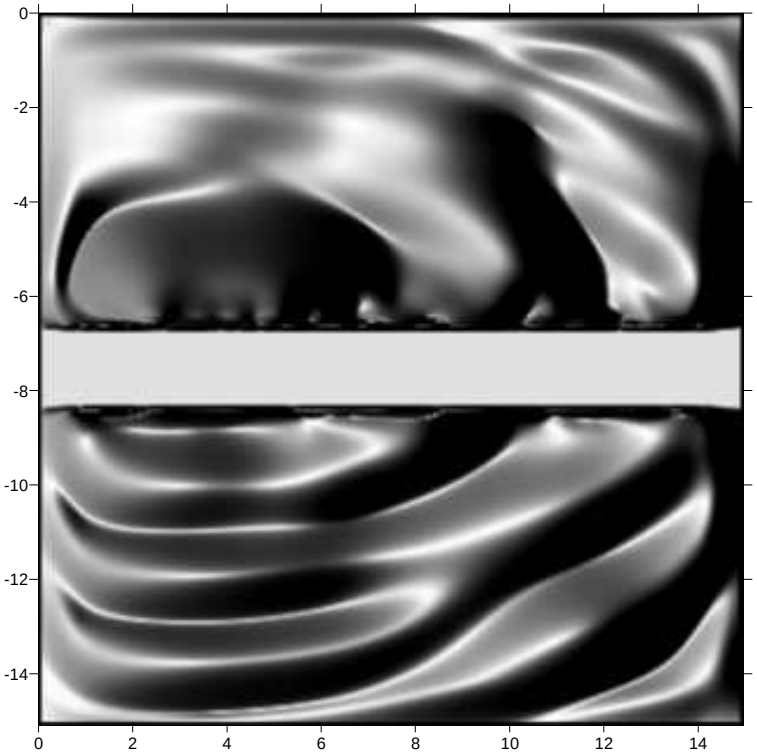


**Figure 67.** Wavefield y=7.5 m snapshot at 0.2 s for adit FD model.

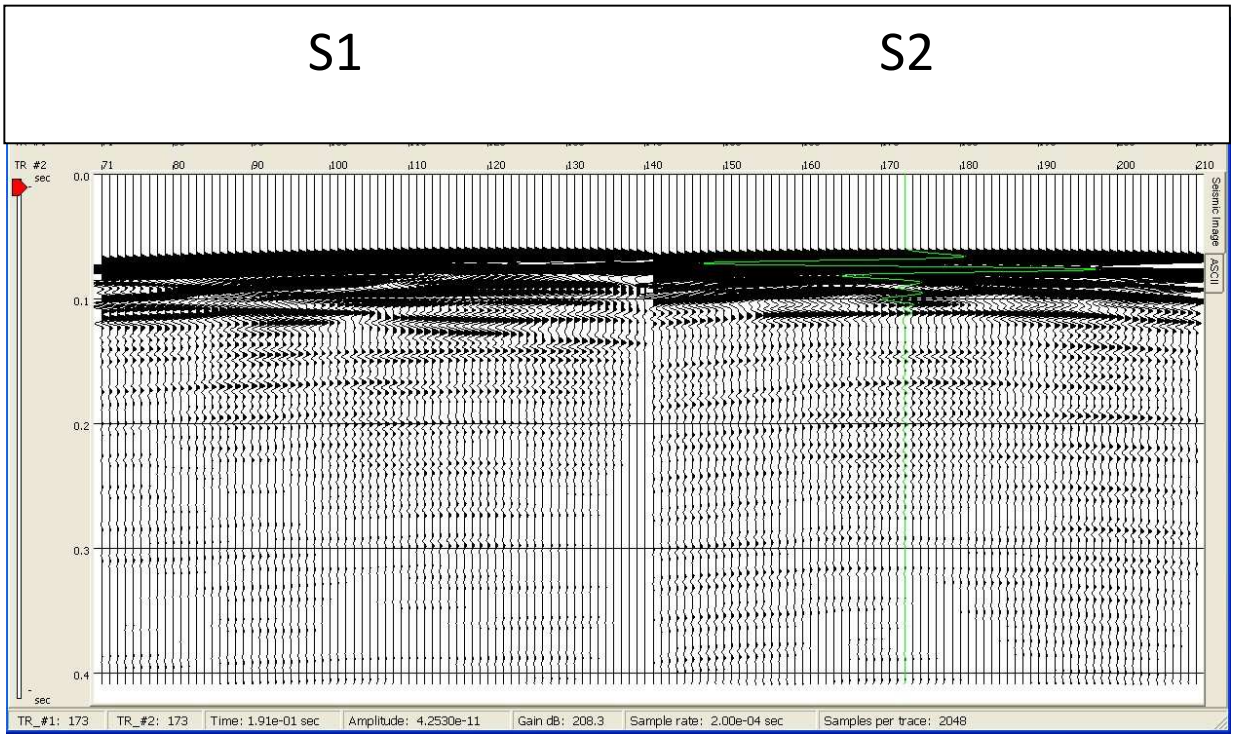


**Figure 68.** FD modeled traces for the adit model. S1 profile aligned along the tunnel, while S2 profile is orthogonal to the tunnel at 5 m offset from the central axis.

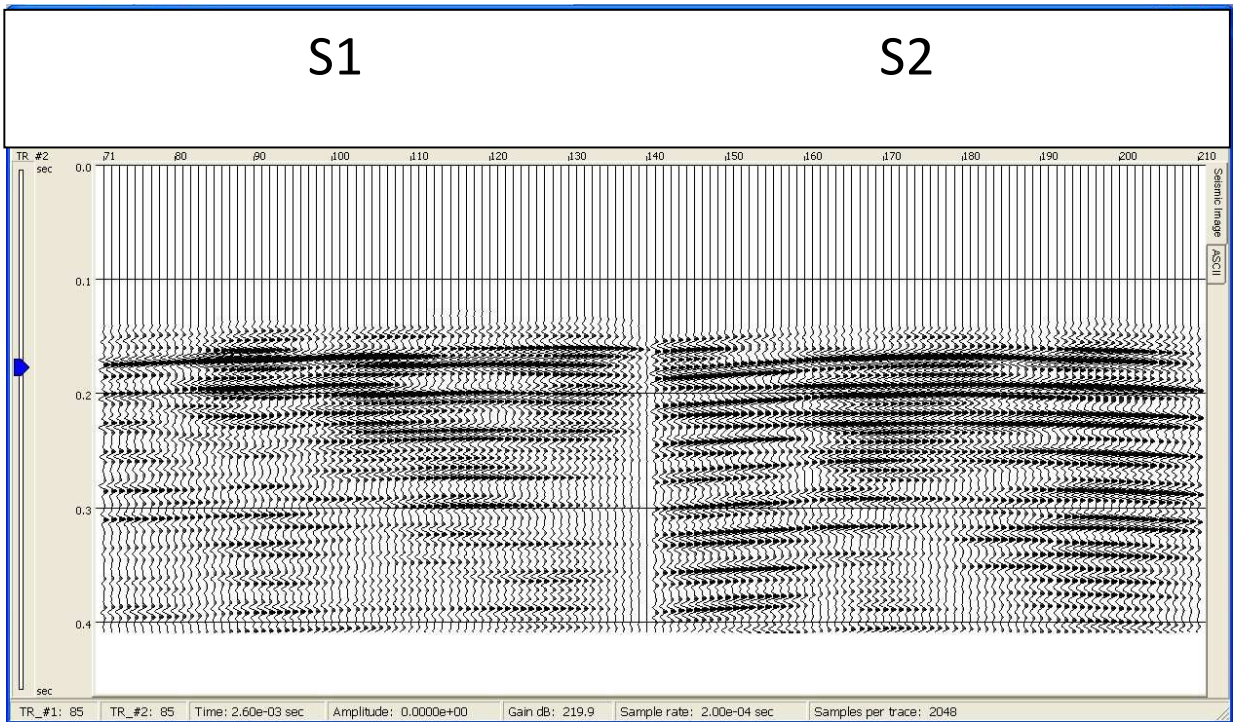


**Figure 69.** Traces from Figure 66 muted before 0.15s.

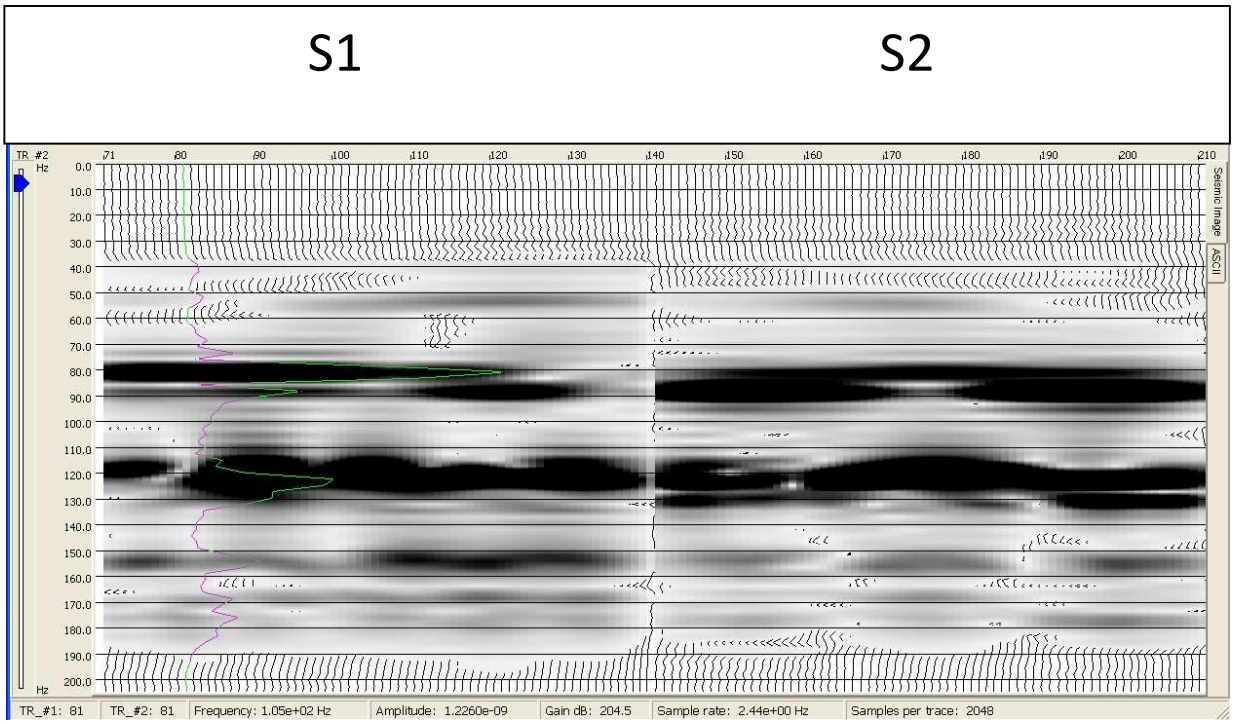


**Figure 70.** Amplitude spectra of traces from Figure 67. Resonant spectra remain constant in frequencies but significantly vary in amplitude.

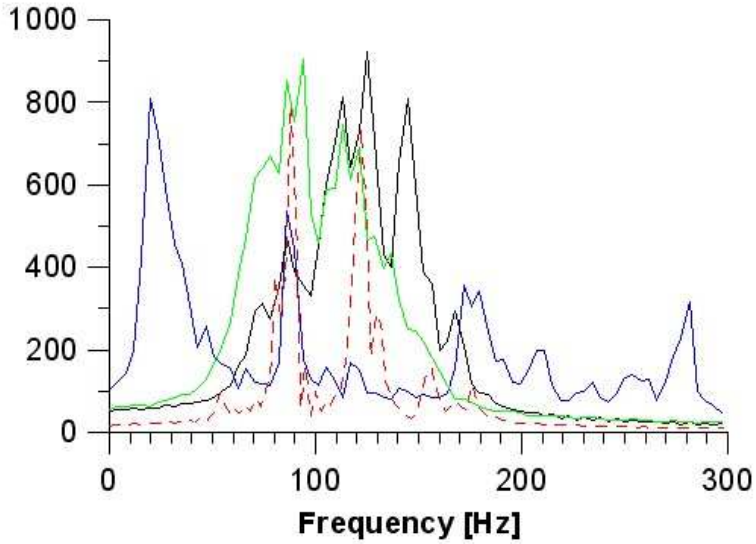


**Figure 71.** Stacked amplitude spectra for: accelerometer data with source in i9 (blue color), accelerometer data with vertical source in P1 (black color), geophone data with vertical source in P1 (green color), and vertical component for S2 profile of FD modeled data (red dashed line).

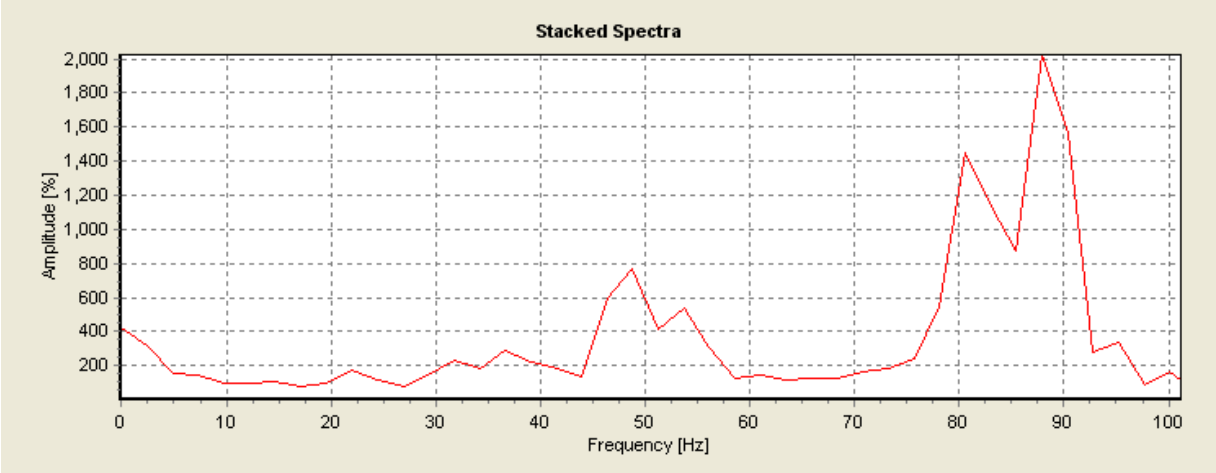


**Figure 72.** Low-frequency part of the modeled spectrum has a small peak at 22 Hz. Compare to Figure 51.

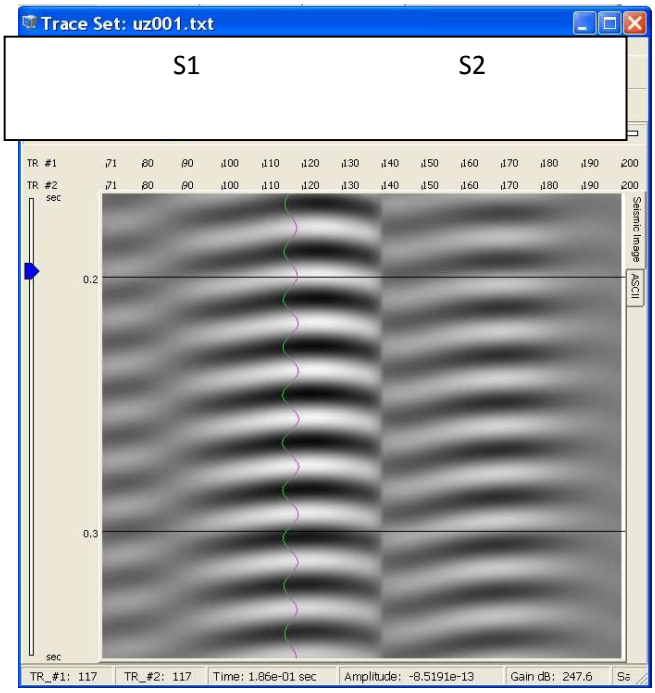


**Figure 73.** FD modeled traces after gating in 0.15 - 0.35 s interval and narrow band-pass filtering around 53 Hz. S1 profile aligned along the tunnel, while S2 profile is orthogonal to the tunnel at 5 m offset from the central axis.

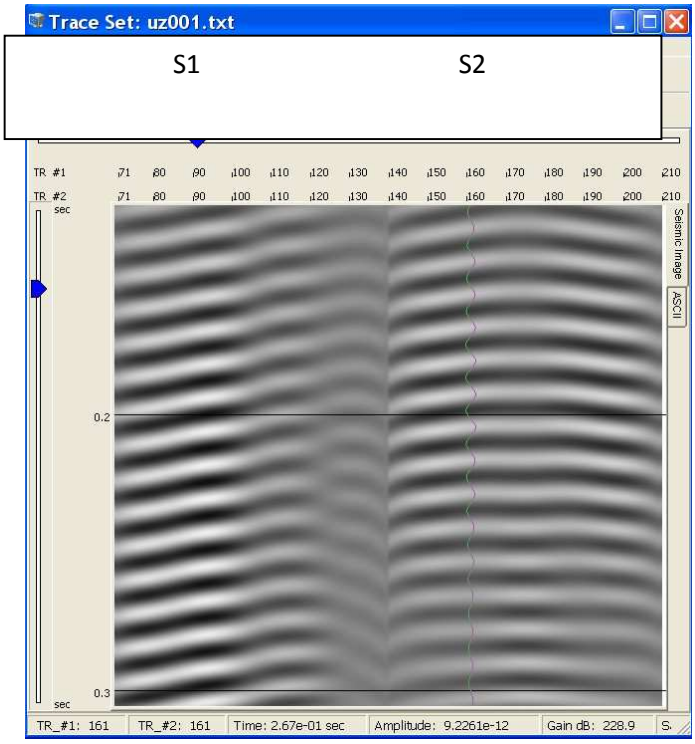


**Figure 74.** Same as on Figure 73 for 88 Hz.

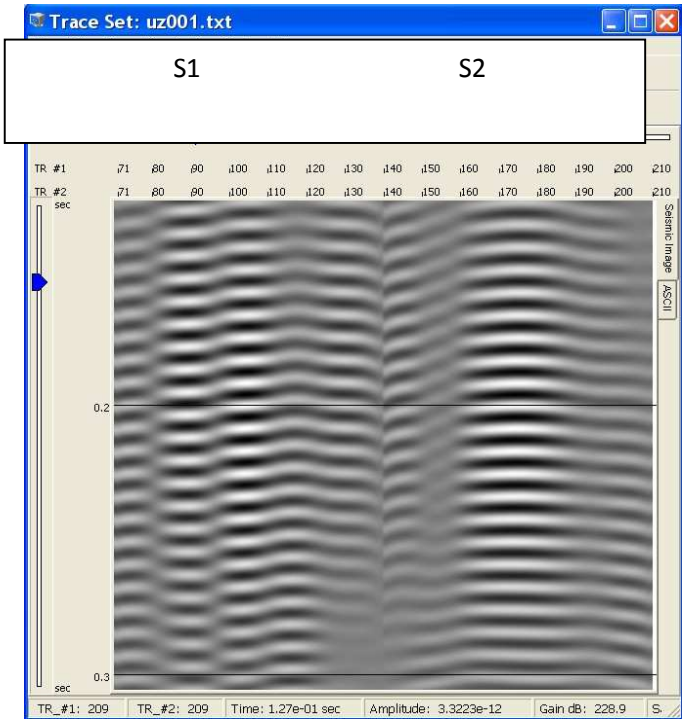


**Figure 75.** Same as on Figure 73 for 118 Hz.

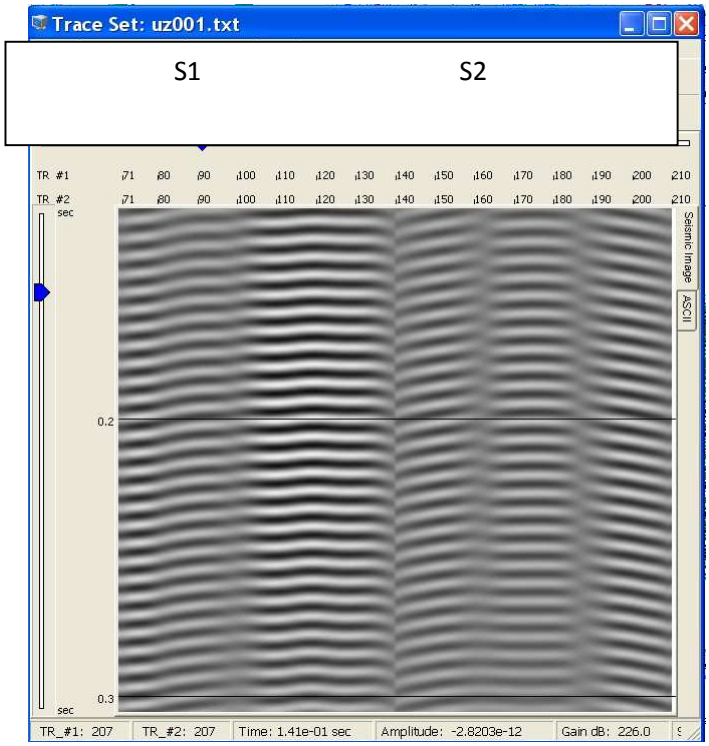


**Figure 76.** Same as on Figure 73 for 154 Hz.

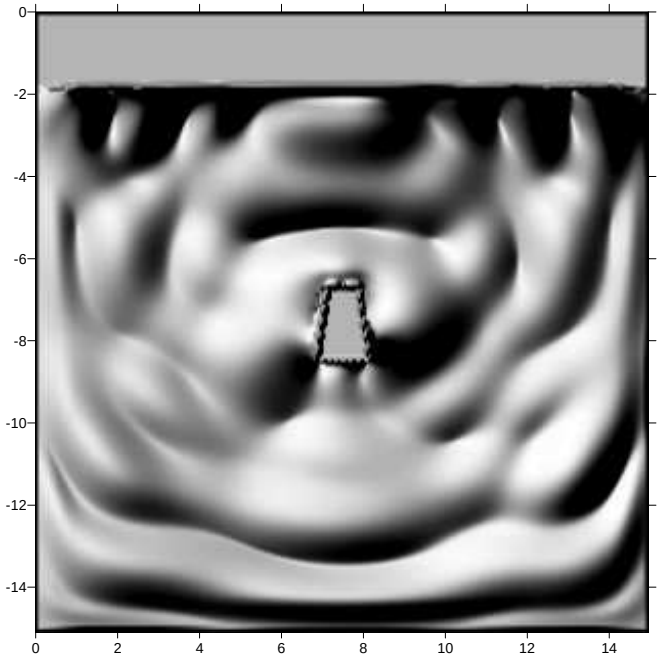


**Figure 77.** Wavefield x=7.5 m snapshot at 0.2 s for adit FD slope model.

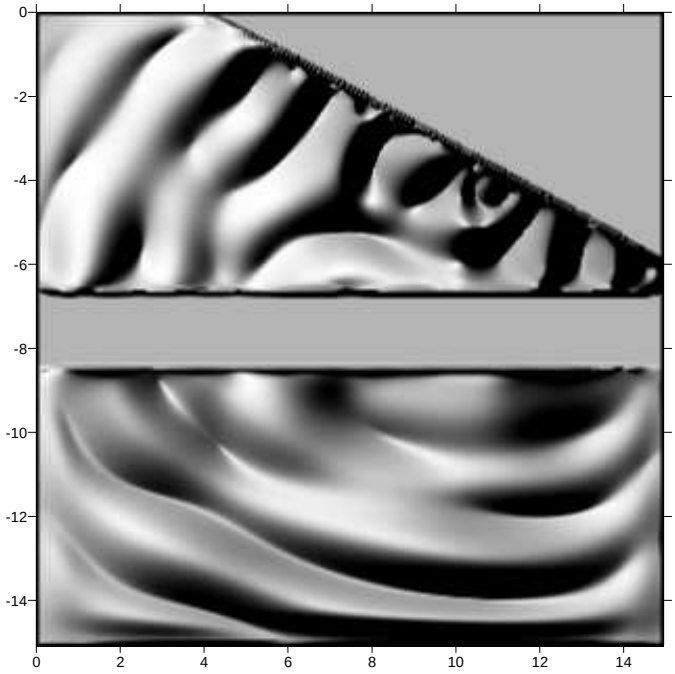


**Figure 78.** Wavefield y=7.5 m snapshot at 0.2 s for adit FD slope model.

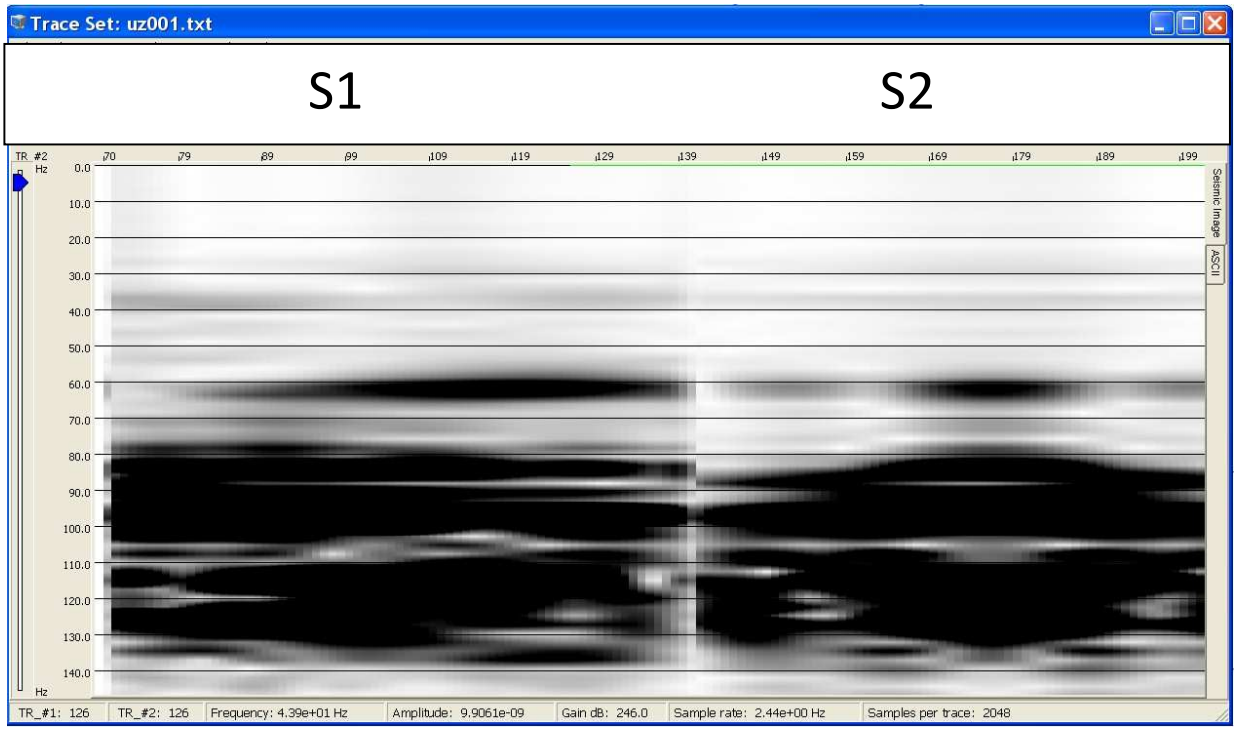


**Figure 79.** Amplitude spectra of traces for the adit model with the slope. Traces were mutes before 0.15 s.

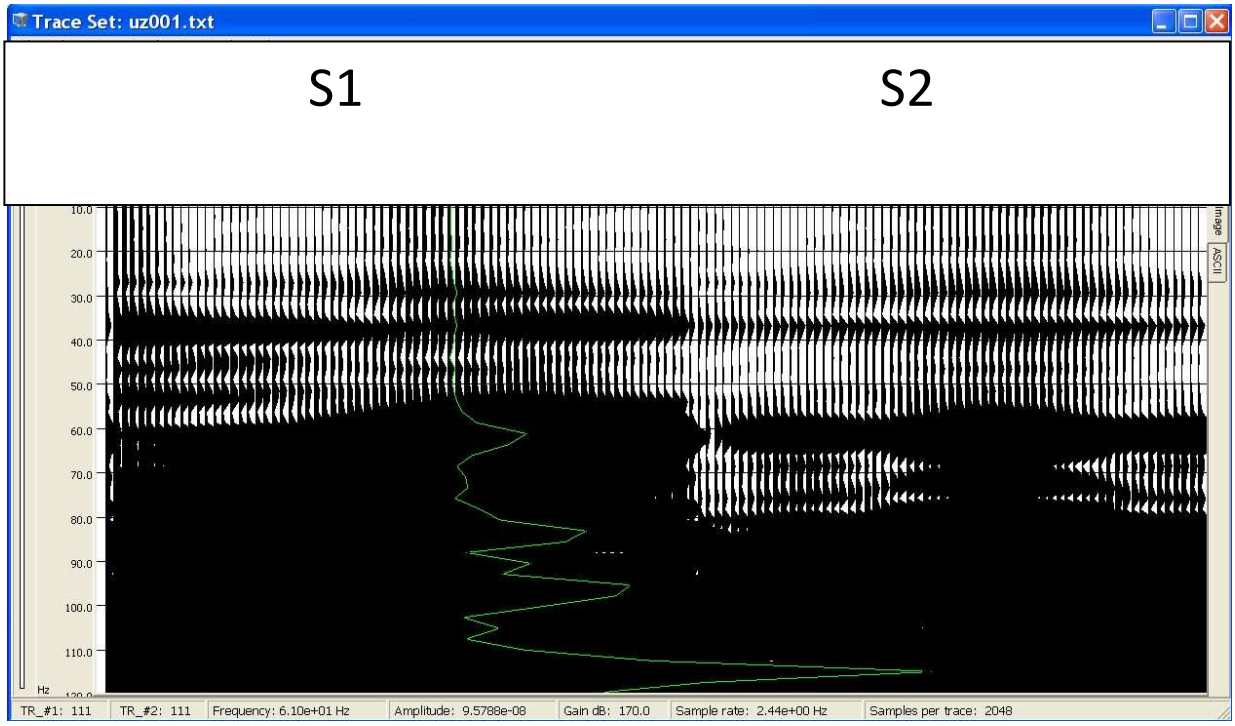


**Figure 80.** Same as on Figure. Note the value of resonant frequency change from 27 Hz to 29 Hz.

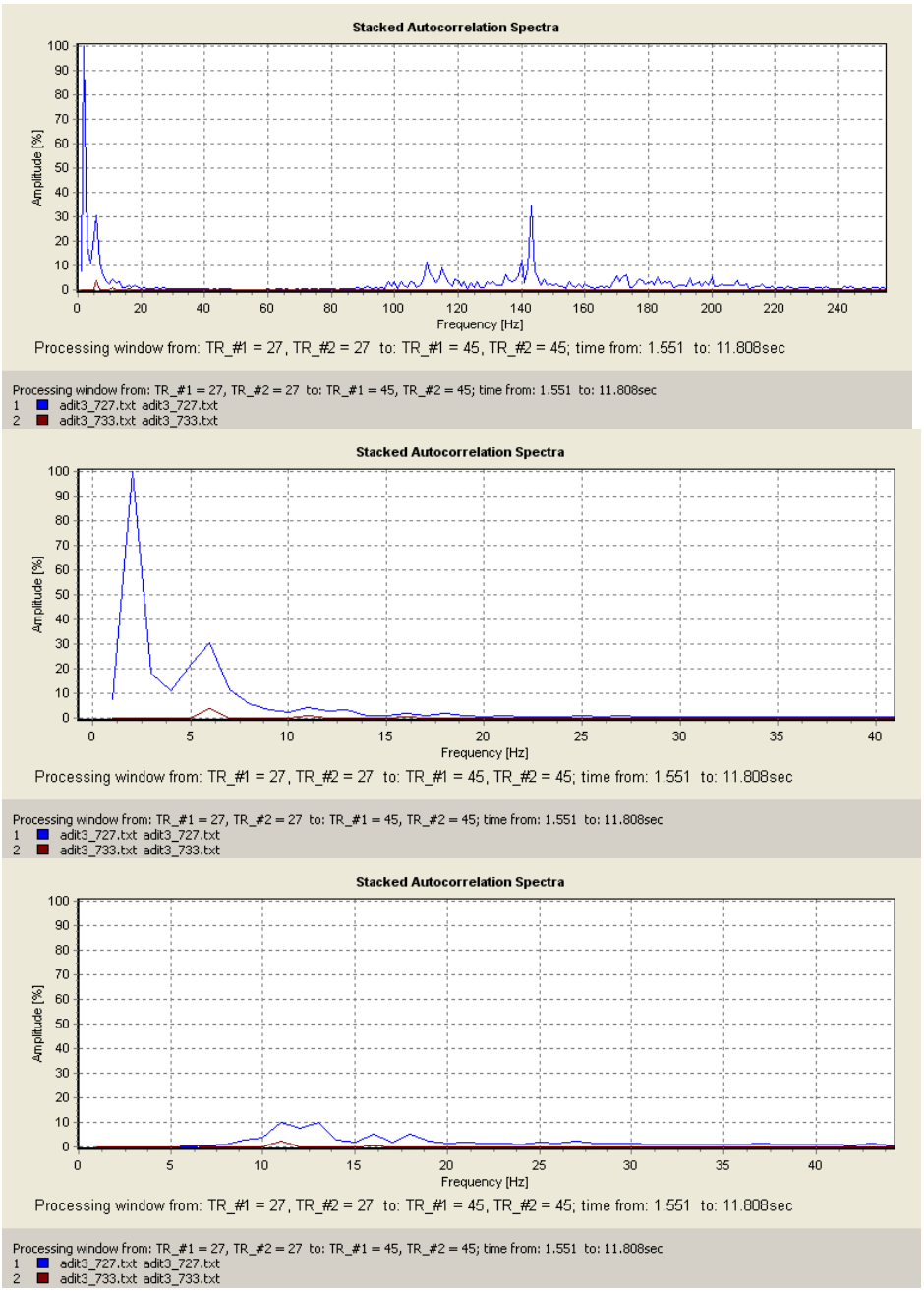


**Figure 81.** Stacked amplitude spectra of geophone records for a person walking in the adit (blue color), and an ambient noise (red color) . Middle panel shows low-frequency part of the full spectrum (upper panel) and the lower panel shows band-passed part around 13 Hz.

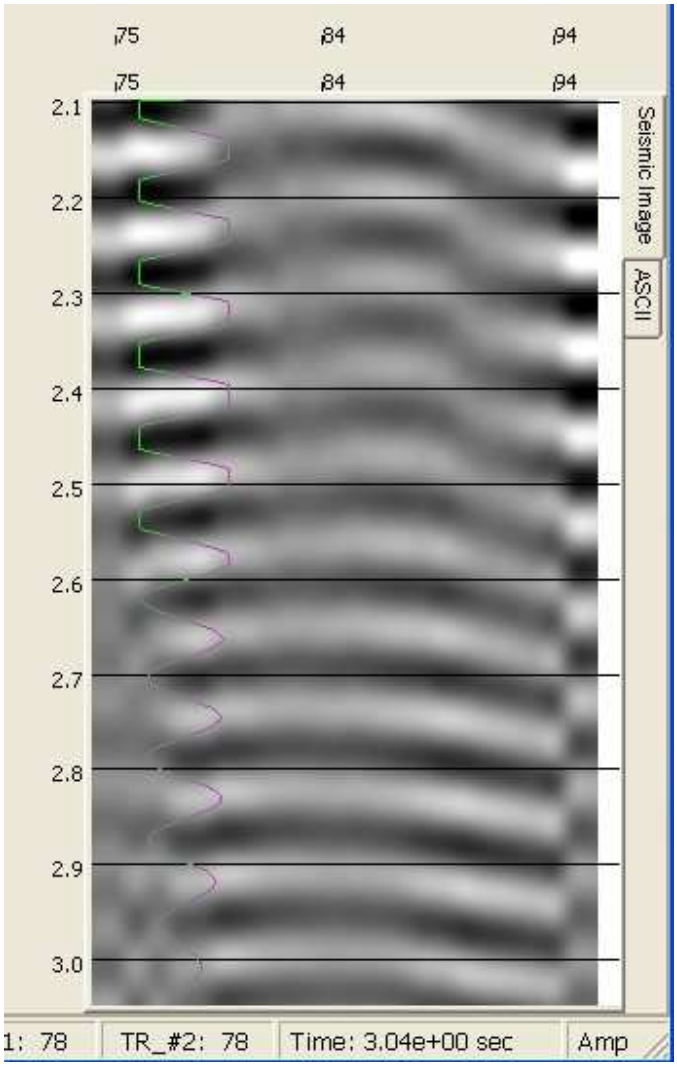


**Figure 82.** Traces from S2 profile band-pass filtered around 13 Hz show that the source of the sound comes from the adit.

## Attachment: Bld.46 Adit history


30 March 2009

To: Rob Connelly

CC: Valeri Korneev

From: Preston Jordan

Re: History of the Building 46 adit

This memo relays my knowledge of the history of the so-called Building 46 adit at your request. The entrance to this adit is located up a short flight of stairs to the east of the southern end of Building 46.

The context for this request is safety planning for an experiment testing the effectiveness of some new geophysical methods at detecting tunnels. This experiment involves installing geophones both inside the tunnel and at the ground surface overlying the tunnel, and generating acoustic waves both at the surface and inside the tunnel. The geophones inside the tunnel will likely be installed via nondestructive means, such as clamping to structural members. Acoustic waves inside the tunnel will likely be generated by hitting the floor and/or structural elements with an intermediate weight hand hammer, for instance weighing approximately two kilograms.

As entry into the adit and interaction with its structural support system is part of the experiment, knowledge about the adit's history is a useful component of planning for the safe, as well as efficient, conduct of the experiment.

I have previously transmitted to you copies of three drawings depicting the adit that I located in the Facilities Division engineering drawing files years ago. You have made multiple copies of these drawings for the project and your files, and returned a set of copies to me.

The earliest drawing concerns provision of support for an existing, unsupported adit. The date of this drawing suggests the adit was excavated prior to the founding of LBNL, then known as the Radiation Laboratory, in the 1930's.

Oral history from Harold Wollenburg, a former research geologist in the Earth Sciences Division, suggested that the adit was excavated to enhance flow from a naturally occurring spring at the site. Wollenburg reported this was common practice in the area at the end of the 19$^{th}$ and beginning of the 20$^{th}$ century, when Berkeley's entire water supply was locally derived. This

perspective is supported by the correlation of Building 46 and former Building 71 adits with spring locations mapped in the late 19th century. It is further supported by discovery of the geologic structure responsible for both these springs, which is the low point of a contact between overlying relatively permeable fractured and disarticulated translational/rotational slide deposits comprised of Moraga Formation volcanic rocks overlying relatively impermeable sedimentary rock of the Orinda Formation.

As mentioned, the oldest drawing extant drawing to my knowledge showing the Building 46 adit presents a cross section through an unsupported adit with a plan for providing timber support. The section indicates both the entrance and deepest portion of the adit have been partially filled by material collapsed either in whole or part from the roof. According to the drawing, the portion of the adit shallower than the collapsed material at the back was to be supported with timber sets with intervening lagging. The rear, partially collapsed section of the adit was to remain unsupported. Inspection of the current adit walls suggests these timber sets were installed and the rear portion of the adit was left unsupported.

This drawing indicates the reason for upgrading this structure was to provide a floor vault in the deepest supported portion of the adit for storing films from the Cyclotron, presumably recording particle tracks before and after collisions. Oral history suggests these films were subject to additional exposure by cosmic rays, and therefore storing them in the adit would better preserve them.

The next set of drawings showing the adit concerns its resupport. One drawing documents failure areas of the timber lagging. Two resupport strategies are presented, one involving removal of the timbers and installation of an elliptical steel liner, and the other bracketing the timber sets with angle steel, replacing the wood lagging with concrete lagging, and installing a floor drain and concrete floor. Inspection of the Building 46 adit indicates the second strategy was implemented, and subsequently covered in shotcrete at an undetermined date.

The next activity in the adit according to Harold Wollenburg was its retrofit for monitoring ground movements as part of an accelerator site study in the 1970s. Mr. Wollenburg participated in the installation and reading of a mercury manometer in the supported portion of the adit and of a plumb bob hanging from the ground surface into the adit via a steel-cased vertical shaft advanced from the surface to a location approximately 100 feet into the adit for the purpose. The readings from these instruments indicated the hillside moved up and out of slope during the rainy season and “relaxed” back during the dry season.

My engagement with the adit commenced approximately 1992 at the time of my initial involvement with the Environmental Restoration Program (ERP). I was tasked with understanding the geologic structure of the area due to the presence of a groundwater plume of chlorinated aliphatic hydrocarbons (VOCs) in the vicinity. I entered the adit to determine was rock types might be exposed. If my recollection is correct, I found two core holes, one angling

down through the shotcrete and concrete lagging on the south side wall and the other through the concrete floor. These holes were both a considerable distance into the supported section of the adit. The boring through the floor was partially filled with water, presumably groundwater. Both holes encountered the contact between the volcanic materials and the Orinda Formation, and provided useful data points in the formulation of the geologic model of the area.

Note at this time, and up until the mid-90s, this volcanic material was taken to be the Moraga Formation, rather than landslide deposits derived from the Moraga Formation. The latter interpretation emerged in the mid to late 90's based upon a variety of observations and various chains of reasoning.

At the time of the 1992 inspection, I observed the back portion of the adit was unsupported and partially collapsed during this inspection. This could be observed from the safety of the rear area of the structurally supported section adjacent to the floor vault. Corrugated metal sheets partitioned off the unsupported section beyond, but these could be moved aside to view this section. All of the observable material and exposures in this unsupported section were comprised of sedimentary rock of the Orinda Formation. I also observed the based of the vertical shaft with the plumb bob still present during my 1992 inspection of the adit.

The geologic information garnered from the 1992 inspection indicated that the contact between the volcanic material and the underlying Orinda Formation dips slightly out of slope, intersects the invert of the adit approximately midway along its length and the ceiling (also known as the "back" in tunneling terms) of the adit in the supported section near its furthest extent.

I believe after my 1992 inspection of the adit for geologic investigation, a discussion ensued with EHS personnel concerning the appropriate level of control regarding access to the adit. One outcome was posting the rear, unsupported section of the adit as a confined space. A sticker communicating this was affixed to the northernmost corrugated metal sheet partitioning off this area. I do not recall the rest of the adit being designated a confined space at that time, although I have some recollection the entry door may have been locked where it wasn't previously. It is also possible these actions were taken after the 1993 ERP activities in the adit described below based upon some weakness in my recollection of the timing.

Despite oral history indicating the adit was created to enhance groundwater flow for local water supply, no groundwater appears to flow into or out of the adit. This is interpreted as due to the installation of a subdrain running along the east side of Building 46 in the alleyway between the adit and the building. This subdrain intersects the same contact as the adit, but at a lower elevation (the contact dips out of slope in this location). This subdrain is capturing considerable groundwater, with the amount fluctuating seasonally. Consequently, it appears this subdrain has lowered the groundwater table below the elevation of the adit invert. Note the subdrain was likely installed during repair and mitigation of the 1973 landslide to the north of adit. This landslide moved the northern half of Building 46 approximately a half meter west.

The ERP subsequently decided to drill holes inside the adit to further characterize the location of the contact between the . The purpose of these wells was to further characterize the VOC groundwater plume. A company specializing in portable hydraulic drilling and well construction was contracted for this work with me as the attending geologist. Two borings were drilled in 1993. Well casings were installed in these borings to collection of groundwater samples as a secondary objective. My recollection is that no backfill was installed around these well casings. The wells were designated SB46adit-93-G1 and SB46adit-93-G2. I recall generating logs of these borings recording the geologic observations and perhaps the well construction. If these logs exist, David Baskin in EHS's Environmental Services Group either have them or know how to access them. In addition groundwater samples were collected from the wells and water level likely measured. Again, David Baskin would be able to provide this data if you are interested.

Both borings were drilled and wells installed without incident. During tear down and removal of the drill rig on the second boring, though, a tray running along the south structural support wall of the adit was disturbed. Mercury was subsequently observed pooling on the floor of the adit in the vicinity of this second boring (although it did not come near to entering the boring). All personnel evacuated the adit, and I contacted emergency services. The LBNL Fire Department and one or more personnel from the Environment, Health and Safety Division (EHS) arrived on the scene.

Despite knowledge from Harold Wollenburg concerning the historic presence of a mercury manometer in the adit, no one including myself thought to inspect for its presence ahead of well drilling. Upon observing the mercury on the tunnel floor subsequent to upset of the tray on the wall, I immediately realized that the manometer was still present and at least partially filled.

A hand held monitor was used by one of these personnel to measure the concentration of mercury vapors in the adit. The concentration was found to be too high to allow entry of drilling personnel to finish retrieving the drill rig. The adit and drill rig were subsequently decontaminated by personnel from or under the supervision of the EHS Division over the next few days. As part of this remediation, an approximately one pint bottle perhaps one-third filled with mercury was found at one end of the manometer and removed. The drilling crew returned after completion of this work and retrieved their equipment.

After 1993, I do not recall physically entering the adit. My next significant discussion concerning the adit occurred in 2007 while consulting on the prospective Next Generation Light Source (NGLS) tunnel. In this capacity I was put in contact with Dick McDonald, an engineer at SLAC National Accelerator Laboratory involved with the Linac Coherent Light Source project, which involved various styles of tunnel.

The Building 46 adit was discussed during my conversation with Mr. McDonald. He recommended constructing a bulkhead partitioning the supported and unsupported sections of the

adit, and injecting a low-strength concrete (sometimes called controlled density fill) through the bulkhead to fill the unsupported section.

I did not inquire why this engineer made this recommendation as it was apparent to me that leaving an unsupported void in the subsurface of the lab was not best practice. On 5 June 2007 I sent this recommendation to the Work Request Center via email. Fred Angliss of the Facilities Division subsequently contacted me by phone to discuss the issue. He concluded that the lab would not take the recommended course of action. The status quo would remain.

This is the sum of my knowledge and memory of the history of the Building 46 adit at this time. If you have further questions, please feel free to contact me.